



Contents lists available at ScienceDirect

# International Journal of Applied Earth Observations and Geoinformation

journal homepage: [www.elsevier.com/locate/jag](http://www.elsevier.com/locate/jag)



## Artificial intelligence-based software (AID-FOREST) for tree detection: A new framework for fast and accurate forest inventorying using LiDAR point clouds

F.R. López Serrano <sup>a,b,\*</sup>, E. Rubio <sup>b,c</sup>, F.A. García Morote <sup>a,b</sup>, M. Andrés Abellán <sup>a,b</sup>, M.I. Picazo Córdoba <sup>b</sup>, F. García Saucedo <sup>b</sup>, E. Martínez García <sup>d</sup>, J.M. Sánchez García <sup>e</sup>, J. Serena Innerarity <sup>e</sup>, L. Carrasco Lucas <sup>f</sup>, O. García González <sup>f</sup>, J.C. García González <sup>f</sup>

<sup>a</sup> Higher Technical School of Agricultural and Forest Engineering, University of Castilla-La Mancha, Campus Universitario s/n, 02071 Albacete, Spain

<sup>b</sup> Renewable Energy Research Institute (Environment and Forest Resources), University of Castilla-La Mancha, Campus Universitario s/n, 02071 Albacete, Spain

<sup>c</sup> Applied Physics Department, University of Castilla-La Mancha, Campus Universitario s/n, 02071 Albacete, Spain

<sup>d</sup> Department of Forest Ecology and Management, Swedish University of Agricultural Sciences, Skogmarksgränd 17, 901 83 Umeå, Sweden

<sup>e</sup> Naturaleza y Tecnología de la Mancha, S.L. (NATURTEC), Polígono Industrial Romica, C/ 1, Parcela 199 Nave E2, Apartado Correos 8138, 02080-Albacete, Spain

<sup>f</sup> Digital Elevation Models (DIELMO 3D), Plaza Vicente Andrés Estellés N° 2 Bajo, 46950-Xirivella, Valencia, Spain



### ARTICLE INFO

#### Keywords:

Mobile laser scanner  
Artificial intelligence  
Automatic tree detection  
Ecosystem visual complexity index  
Tree stem volume  
Forest stand parameters

### ABSTRACT

Forest inventories are essential to accurately estimate different dendrometric and forest stand parameters. However, classical forest inventories are time consuming, slow to conduct, sometimes inaccurate and costly. To address this problem, an efficient alternative approach has been sought and designed that will make this type of field work cheaper, faster, more accurate, and easier to complete. The implementation of this concept has required the development of a specifically designed software called "Artificial Intelligence for Digital Forest (AID-FOREST)", which is able to process point clouds obtained via mobile terrestrial laser scanning (MTLS) and then, to provide an array of multiple useful and accurate dendrometric and forest stand parameters. Singular characteristics of this approach are: No data pre-processing is required either pre-treatment of forest stand; fully automatic process once launched; no limitations by the size of the point cloud file and fast computations.

To validate AID-FOREST, results provided by this software were compared against the obtained from in-situ classical forest inventories. To guaranty the soundness and generality of the comparison, different tree species, plot sizes, and tree densities were measured and analysed. A total of 76 plots (10,887 trees) were selected to conduct both a classic forest inventory reference method and a MTLS (ZEB-HORIZON, Geoslam, Ltd.) scanning to obtain point clouds for AID-FOREST processing, known as the MTLS-AIDFOREST method. Thus, we compared the data collected by both methods estimating the average number of trees and diameter at breast height (DBH) for each plot. Moreover, 71 additional individual trees were scanned with MTLS and processed by AID-FOREST and were then felled and divided into logs measuring 1 m in length. This allowed us to accurately measure the DBH, total height, and total volume of the stems.

When we compared the results obtained with each methodology, the mean detectability was 97% and ranged from 81.3 to 100%, with a bias (underestimation by MTLS-AIDFOREST method) in the number of trees per plot of 2.8% and a relative root-mean-square error (RMSE) of 9.2%. Species, plot size, and tree density did not significantly affect detectability. However, this parameter was significantly affected by the ecosystem visual complexity index (EVCI). The average DBH per plot was underestimated (but was not significantly different from 0) by the MTLS-AIDFOREST, with the average bias for pooled data being 1.8% with a RMSE of 7.5%. Similarly, there was no statistically significant differences between the two distribution functions of the DBH at the 95.0% confidence level.

Regarding the individual tree parameters, MTLS-AIDFOREST underestimated DBH by 0.16 % (RMSE = 5.2 %) and overestimated the stem volume (V<sub>t</sub>) by 1.37 % (RMSE = 14.3 %, although the BIAS was not statistically

\* Corresponding author at: Higher Technical School of Agricultural and Forest Engineering, University of Castilla-La Mancha, Campus Universitario s/n, 02071 Albacete, Spain.

E-mail address: [fco.lopez@uclm.es](mailto:fco.lopez@uclm.es) (F.R. López Serrano).

significantly different from 0). However, the MTLS-AIDFOREST method overestimated the total height (Ht) of the trees by a mean 1.33 m (5.1 %; relative RMSE = 11.5 %), because of the different height concepts measured by both methodological approaches. Finally, AID-Forest required 30 to 66 min per ha<sup>-1</sup> to fully automatically process the point cloud data from the \*.las file corresponding to a given hectare plot. Thus, applying our MTLS-AIDFOREST methodology to make full forest inventories, required a 57.3 % of the time required to perform classical plot forest inventories (excluding the data postprocessing time in the latter case). A free trial of AID-Forest can be requested at dielmo@dielmo.com.

## 1. Introduction

Forest inventories are essential to accurately estimate different forest stand parameters that are key to implementing sustainable forest management. They are also fundamental in ecosystem research, carbon accounting, and ecophysiology, because forest stand parameters allow the current condition of forests to be characterised and thus, provide a reliable basis for management planners to make more informed decisions. However, performing classical forest inventories involving the use of callipers, tapes, and hypsometers, well conducted sampling, or full inventories, is the most expensive component in forest management plans and is hard, time-consuming, and tedious work.

Geomatic techniques, such as airborne Light Detection and Ranging (LiDAR) technology, have been used to estimate the parameters of forest stands for just over two decades (Næsset, 2002; Nelson et al., 2003). However, inaccurate results are sometimes obtained because aerial LiDAR is unable to capture stem information. On the contrary, static terrestrial laser technology (TLS) can collect information from stems, although this technology has not yet been able to replace classical methods, despite the incomparable structural information it is able to capture.

TLS can obtain a 3D representation of vegetation with an accuracy of up to 1 mm (Van Leeuwen and Nieuwenhuis, 2010), while also directly obtaining the diameters and heights of vegetation. The main drawback of TLS systems is the ‘hiding effect,’ which could be corrected if several LiDAR systems are employed or if several different positions on the plot are used rather than a single location. However, this would make the field data collection slower and more expensive (Bauwens et al., 2016).

Mobile terrestrial laser scanning (MTLS) tools are also currently being used for different applications such as the measurement of buildings, both indoors and outdoors (Chen et al., 2021; Rodriguez-Martin et al., 2018; Russakim et al., 2018; Zheng et al., 2018), recreating historical sites in virtual and augmented reality (Barba et al., 2019; Patrucco et al., 2019), mining and caves (Dewez et al., 2017; Liang et al., 2021; Raval et al., 2019), detecting pole-shaped objects while scanning roads (Cabo et al., 2014; Shokri et al., 2019), traffic signs (Yang et al., 2013), lane markings (Rastiveis et al., 2020), highway cross-slopes (Shams et al., 2018), and in accident events and sketches (Topolšek et al., 2019). This is made possible thanks to the ability of MTLS to accurately generate point clouds along with appropriate software to measure them. The most recent application for this technology is for forest inventories, where point clouds are useful resources to get forest structure, i.e., diameter at breast height (DBH), total height, volume, and other parameters of interest, including georeferencing the position of the trees.

The manual extraction of forest stand parameters from the point cloud is not an operational option because it is very labour intensive and time consuming (Safaie et al., 2021) and in fact, there are very few manual applications, and they are focused on reduced forest stand extensions and simplified forest structures (Bogdanovich et al., 2021; Holopainen et al., 2014). Besides, the automated methods for extracting the forest stand parameters from point clouds can be grouped as: (i) point-based, i.e., the algorithm uses points to directly extract the tree parameters (Liang et al., 2014); (ii) grid-based, in which point clouds are grid-converted, a technique also referred to as rasterisation (Safaie et al., 2021); and (iii), other grid-based methods in which point clouds are

converted with a voxel grid (Heinzel and Huber, 2017; Hosoi et al., 2013).

In general, both manual and automatic methods determine tree parameters from point clouds by following these three steps: (1) prior estimation of the digital terrain model (DTM) to standardise the point cloud to the horizontal plane; (2) detection and localisation of the trees; and (3), measurement of the tree parameters of the detected trees. In addition, each step can be tackled with different approaches (for more details, see Othmani et al. (2011)), thus, for example, (i) a DTM can be obtained via the lowest Z-value, or by triangular irregular network model; (ii) the tree detection can be based on Hough transform, on clustering and fitting circles or cylinders, or on point density raster analysis; and (iii) the measurement of tree parameters such as total height can be done by calculating the difference between the DTM and digital surface model (DSM) at the point where a tree is, or the DBH can be obtained by adjusting a circle 1.30 m above ground, as described in Safaei et al. (2021).

Focusing on tree detection algorithms, different studies have used the 2D Hough transform to detect and measure the DBH of trees after normalisation to an elevation of 0 m, discounting the digital terrain model of the point cloud (Simonse et al., 2003). In a similar but improved method, Gorte and Pfeifer (2004) and Gorte and Winterhalder (2004) used a 3D mathematical morphology. Pfeifer and Winterhalder (2004) modelled transversal tree sections with free-form curves. In turn, Othmani et al. (2011) described an approach for automatically detecting and isolating trees and estimating their DBH. This used the open-source software called Computree, an innovative approach based on a clustering methodology, as well as Hough transform for tree detection, followed by a skeletonization step to automatically obtain the DBH. Later, Othmani et al. (2013) developed a tool for both homogeneous and heterogeneous forest plantations that can automatically or semi-automatically recognise the species at gender level and measure the tree parameters. Olofsson et al. (2014) used a new method to detect, classify, and measure tree stems based on Hough transform and the Random Sample Consensus (RANSAC) algorithm. In turn, Bauwens et al. (2016) used Computree, along with algorithms from the ONF-ENSAM plugin that are also based on Hough transform (Othmani et al., 2011), and some additional improvements to extract forest parameters from point clouds.

Safaie et al. (2021) used a mixed point and grid-based method to automate a tree inventory along roads by using MTLS. They used both Hough transform and the active contours algorithm on several generated raster images from point clouds. In turn, Mokroš et al. (2021) used the cylinder-based algorithm to detect trees and measure their DBH. Furthermore, Cabo et al. (2018a) developed an automatic method to identify tree stems based on the isolation and vertical continuity of stems via an iterative process. Other authors, including Bienert et al. (2007), have also used mathematical morphology techniques (Serra, 1982). They conducted an initial segmentation step consisting of a point cluster search in a cross section of the point cloud, and then verified or discarded all the clusters by analysing the point density in neighbouring cross sections to minimise the probability of false detections. Recently, Hyppä et al. (2020b) described a novel postprocessing algorithm to extract stem curves from scan-line arcs corresponding to individual standing trees. Finally, Vatandaşlar and Zeybek (2021) used machine learning (e.g., the Caret Random Forest classifier for tree detection in the

R package [version 6.0-86]) and innovative algorithms (e.g., ellipse fitting to estimate the diameter of noncircular trees) to more accurately obtain key forest stand parameters.

In this context, the main contribution of this study has been the development of a new software called Artificial Intelligence for Digital Forests (AID-FOREST) that rasterizes point cloud slices at different heights from the ground and makes use of artificial intelligence to identify and measure tree sections, extract the location of the trees and measure the most relevant tree and forest stand parameters required for sustainable forest management. AID-FOREST solves the main problems faced by currently used algorithms in terms of high processing complexity and, therefore, we can say that it represents a major advance over existing procedures. It was designed to be fully operational and efficient, so that no human intervention is required during processing, no preprocessing of the point cloud or the area to be analysed is required, and it can work with point cloud files of large areas, or link multiple files to cover large areas. Parameters such as stem volume are measured rather than estimated, as occurs in most current software and algorithms. Finally, it provides results at both individual and area level. The two main objectives of this current work to validate AID-FOREST were (1) to check the ability of the algorithm to detect trees and measure their DBHs at the plot level; and (2) to evaluate the algorithm's success in estimating the DBH, total height, and total stem volume at individual tree level.

## 2. Methodology

### 2.1. Artificial Intelligence for Digital FOREST (AID-FOREST) software description and algorithms

AID-FOREST is a software tool that uses artificial intelligence to analyse LiDAR point clouds coming from the forest to detect trees. These detections can be used to obtain both individual measurements of each tree and stand parameters, as well as statistics relating to the whole study area.

The software isolates trees based on object detection by leveraging an artificial intelligence system that is trained to locate stem sections. This allows much more information to be extracted from the forest system than would be possible using a classical inventory method (either a full inventory or by sampling plots). AID-FOREST adapts easily to any workflow, is easy to use and can automatically detect elements and make decisions based on these findings. It is optimised to work with large volumes of data in a short time and provide a comprehensive report of results. However, the current version of the AID-FOREST software is optimised to assess the total volume of individual stems (monopodial branching) but not for multiple stems or branches (sympodial branching).

From the user's point of view, the general workflow that must be followed to obtain both tree and forest stand parameters is shown in Fig. 1. Briefly, once the point clouds of all the plots or stands have been recorded, they should be pre-processed using the manufacturer's specific software to obtain point clouds in LASer (\*.las) format file (clipped to the limits of the plots or stands). Then, the data are fed into the AID-FOREST software. Next, after a simple and fast configuration setup step, the point cloud files are processed to obtain the results output as one \*.shp file each for trees and sections (boxes) and one \*.csv file each at the plot and compartment or stand levels. In addition, normalised cloud files, digital terrain model (DTM), digital surface model (DSM), and digital height model (DHM), will also be obtained.

The internal workflow that AID-FOREST follows is shown in Fig. 2. The general procedure rasterises slices from the point cloud at a certain thickness and at different heights from the ground (both parameters are user defined) and then detects and measures the tree sections. Thus, each MTLS point cloud file (in \*.las format) is imported as input data and processed according to the following steps: (1) calculation of the DTM; (2) computation of the normalized point cloud at a horizontal plane; (3)

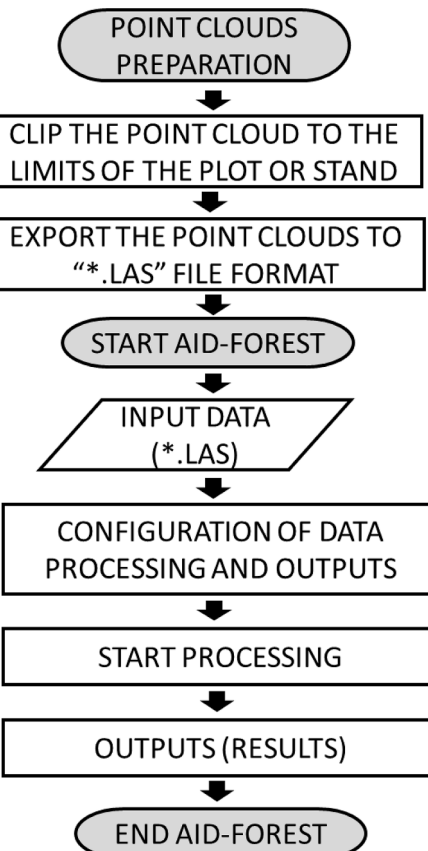


**Fig. 1.** Workflow used to obtain the tree and forest stand parameters using point cloud data, MTLS software, and AID-FOREST software.

rasterization of the normalised point cloud; (4) application of element (tree section) detection algorithms; (5) application of tree detection algorithms; (6) application of tree measurement algorithms; (7) application of crown coverage algorithms for different z-levels; and (8) obtain the data outputs in different formats. These steps are described in detail in the following sections.

#### 2.1.1. Calculation of the digital terrain model and digital surface model.

Because assessment of the main tree parameters is based on measuring different diameters above ground (such as the DBH or the tree volume as a sum of the log volumes of a specific length, etc.) but the terrain is not horizontal or flat, we must first obtain the digital terrain model (DTM). This DTM will then be used to calculate the point cloud normalised to a horizontal plane (see section 2.1.2). The DTM resulted from a raster image created with the minimum height per pixel and removing pixels that did not correspond to the terrain based on a slope criterion. The final DTM is obtained from the interpolation of the raster image. To subsequently assign a height to the detected trees, it is necessary to develop a Digital Surface Model (DSM). Since this DSM is defined on the basis of the normalised point cloud, then the DSM coincides with the Digital Height Model (DHM). Note that in both cases the pixel size was larger than  $1 \times 1$  m, but can be generated with a user-defined pixel size (see "User's Manual" in the Appendix).

#### 2.1.2. Obtaining the point cloud normalised to ground level

The digital terrain model is subtracted from the complete point cloud to obtain the point cloud normalised to a horizontal plane. This is, the normalised point cloud is the original point cloud where the Z coordinate (elevation) is transformed on Z', being  $Z' = Z - \text{DTM}$ . Thus, when we cut the slices at different heights, they will correspond to the correct aboveground heights. This normalised point cloud will be used in steps

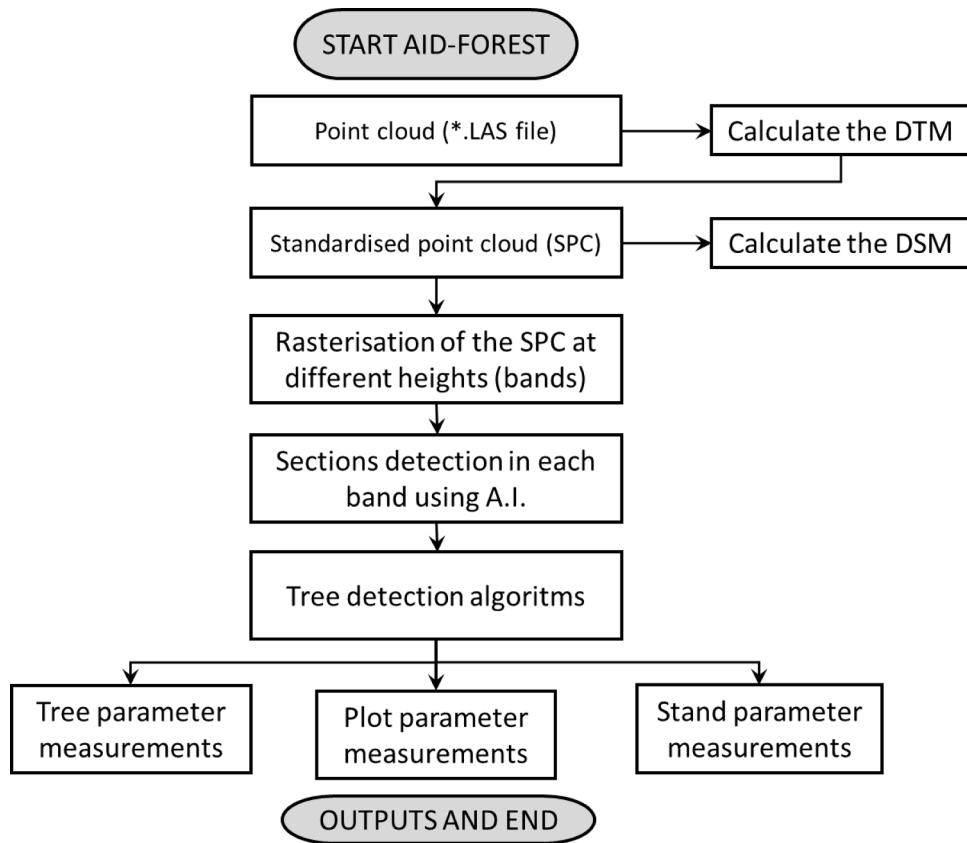


**Fig. 2.** The internal workflow of AID-FOREST. AI: artificial intelligence.

described below.

#### 2.1.3. Rasterisation of the normalised point cloud

Raster images are created at different heights of the normalised point cloud, defined in the ‘List of heights to process’ parameter (see the ‘Configuration Menu’ in the Appendix). These raster images are created by cutting the point cloud at the specified height into slices of Z thickness (‘Z Resolution for detection,’ a user defined parameter described in the Appendix). Thus, a multiband image is obtained in which each band corresponds to a cross section of the point cloud at the height specified in the configuration menu. Rasterization is also user defined, although it is advisable to use a pixel size of  $1 \times 1$  cm to obtain a smooth, well-defined cross section of the stem. These raster images are then used in the next step to detect trees using artificial intelligence-based object detection.

#### 2.1.4. Element (tree section) detection algorithms

The cross sections of stems define the circumferences (or similar geometries) that are easily detectable by properly trained artificial intelligence systems. Thus, AID-FOREST detects these elements on each band image using an artificial intelligence-trained model, the TensorFlow Object Detection API ([https://github.com/tensorflow/models/tree/master/research/object\\_detection](https://github.com/tensorflow/models/tree/master/research/object_detection)). This is an open-sourced framework built on TensorFlow that makes it easy to construct, train, and deploy object detection models (Huang et al., 2017). The resulting model, which represents a compilation of the neural network training results (using TensorFlow) and is responsible for identifying elements on an image without the need for human intervention, is the most important element of the AID-FOREST software (Huang et al., 2017). Each element it locates is called a detection and has an associated score (Fig. 3). This parameter indicates the goodness of the detection and ranges from 0 to 1, where scores close to 0 are considered bad detections (likely not stem sections) while those close to 1 are considered good detections (likely stem sections). When setting up AID-

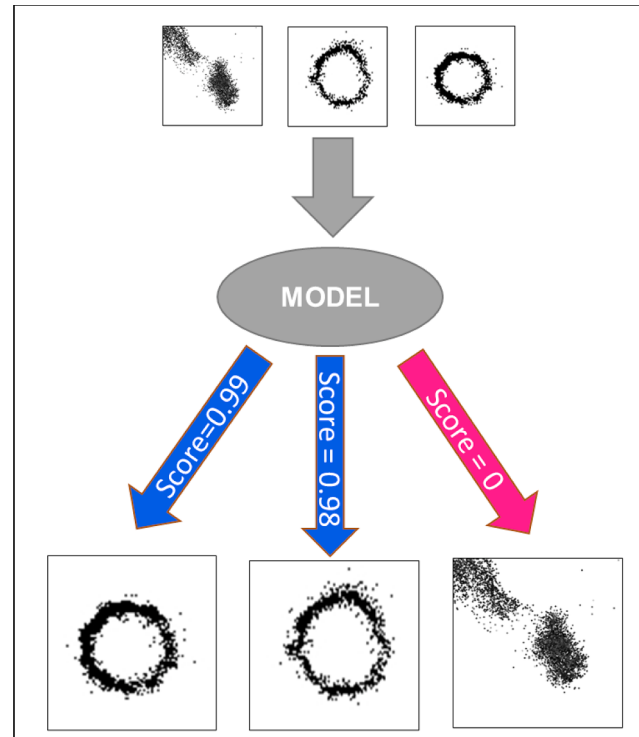


**Fig. 3.** The scheme used for section detection based on an artificial intelligence model and the probability assigned between 0 and 1 (score).

FOREST we must input a user-defined parameter (see the Appendix) to indicate the point at which the score value is considered a stem section.

We used a pre-trained model named ‘faster\_rcnn\_inception\_v2\_feature\_extractor’ (Faster R-CNN; Ren et al. (2015)) to train our custom model. A pre-trained model learns much faster than if it is not trained, because it is based on so-called transfer learning. In addition, Inception V2 architecture is used because it has a good balance between high accuracy and speed among Convolutional Neural Network architecture. A total of 6,167 samples were used, of which 4,921 (*ca.* 80 %) were used to train the model and 1,246 (*ca.* 20 %) to validate the training results. The samples used to train the model were obtained from the manual labelling of log sections from the previously mentioned cross sections of scanned plots or stands taken at different heights.

To optimise performance in the tree section detection process, AID-FOREST splits the raster images into smaller units, adding a buffer to each unit to avoid cutting trees at the edge of the unit. However, this could result in redundant trees, i.e. the same tree being counted twice when present in the buffer of two adjacent units. To solve this problem, a coding is included to eliminate redundant trees (code “-2” in the ID\_GROUP parameter of the boxes file, as shown in the Appendix).

Once the cross sections at plot level are detected (Fig. 4), the images are easy to parametrise with rectangular geometries tangent to the stem (Fig. 5), allowing the diameter of the cross section to be obtained as the average of the sides of the rectangle. Note that the rectangle adjusts over the external border of the circumference into the image. Thus, AID-FOREST contains an input parameter called ‘Offset detection adjust’ (see Appendix) that depends on the bark types of the different tree species and point cloud quality. This parameter usually takes values between – 0.05 and – 0.09 m which correspond to the dispersion (noise) of the point cloud in contact with the stem. Nonetheless, detecting a circumference-like shape does not guarantee that it will be a stem section because other objects such as stones, brush, or artificial objects, etc., can have similar circular sections. Therefore, once the trees are detected we will proceed to determine which groups of detections

will be considered trees, as described below.

### 2.1.5. Tree detection algorithms

The ‘tree’ concept that must be elucidated by the software is based on the multiple sections detected along the vertical position. Thus, when detections at different heights planimetrically overlap by a certain user-defined percentage (the ‘Percentage of Intersection’ parameter described in the Appendix), we can say that they belong to the same object and thereby use them to define and locate a tree. However, to avoid erroneous tree detections (objects other than trees), AID-FOREST requests additional information, namely, that more than ‘n’ sections were detected in the vertical projection (a user-defined number of matches, as shown in Fig. 6 and in the Appendix). If both conditions are fulfilled, these detections are grouped into the same ‘ID\_GROUP’ and are given a tree number (a positive integer). In contrast, when they are not fulfilled, they will be coded as ‘ID\_GROUP = –1’ to denote that are not sections of a tree (see Appendix). In this step, the planimetric position of a tree (X and Y, in m) is considered to be the centroid of the lowest detection of each group.

### 2.1.6. Tree measurement algorithms

After identifying all the detected sections and trees, the following tree variables are calculated (Fig. 7): DBH, diameters ( $d_i$ ) at different heights ( $h_i$ ), the normal section at breast height (ba), total height of the tree (Ht), height where the crown starts (H1v), distance from the ground to the first verticil of branches, and total volume of the stem (Vt).

The DBH (cm) is defined as the diameter at 1.30 m (or as close as possible to 1.30 m) above ground. When there is no detection at 1.30 m, AID-FOREST calculates the mean of the immediate diameters above and below the 1.30 m level; if this is impossible, the diameter of the first lower detected section is used or otherwise, the value of the first upper section is used. The height at which the DBH is measured is always shown in the tree outputs file.

$ba (m^2)$ , is the basal area at breast height, calculated as:

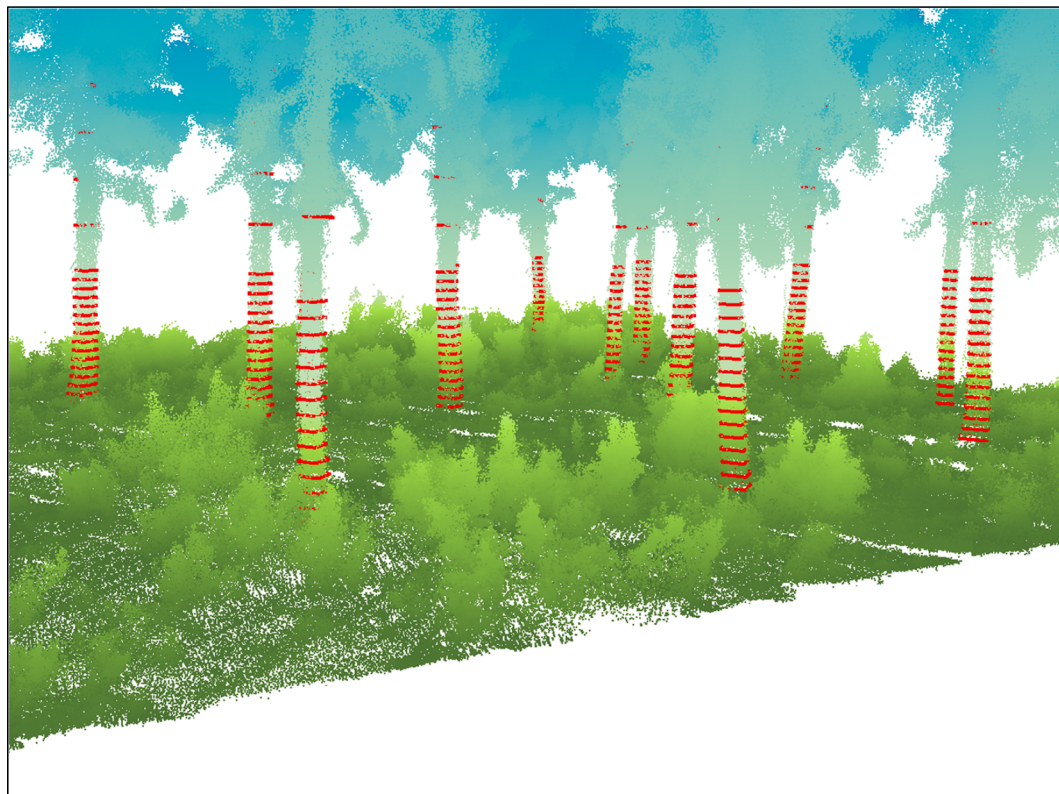
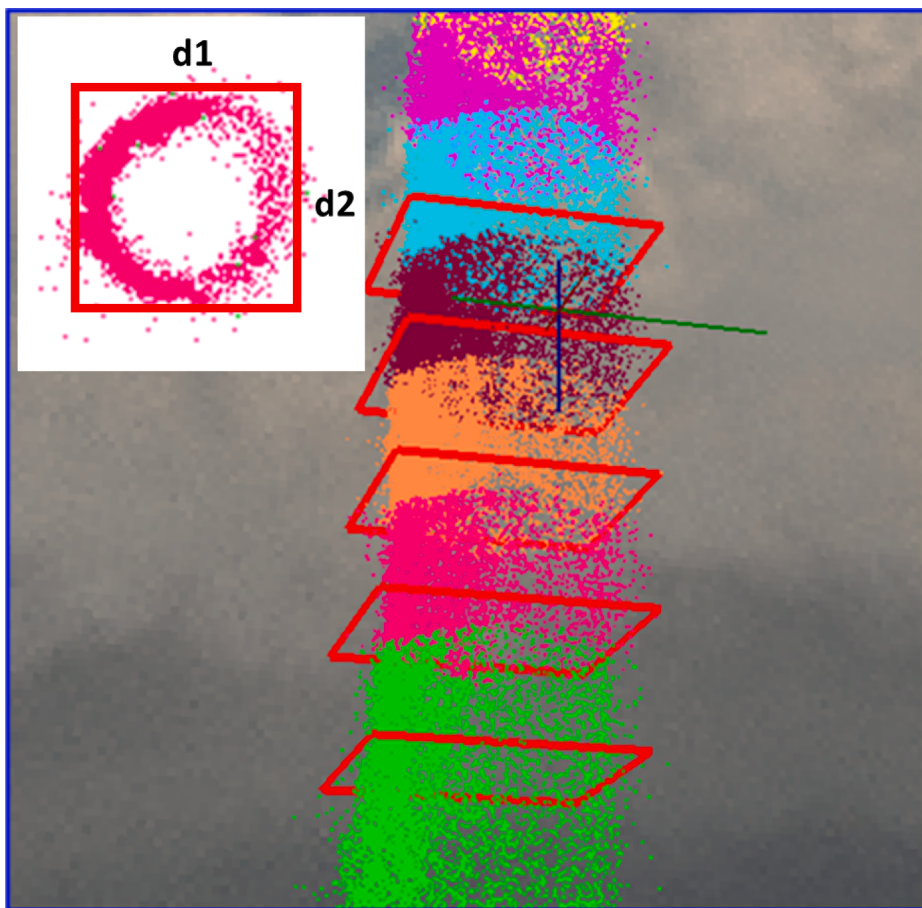
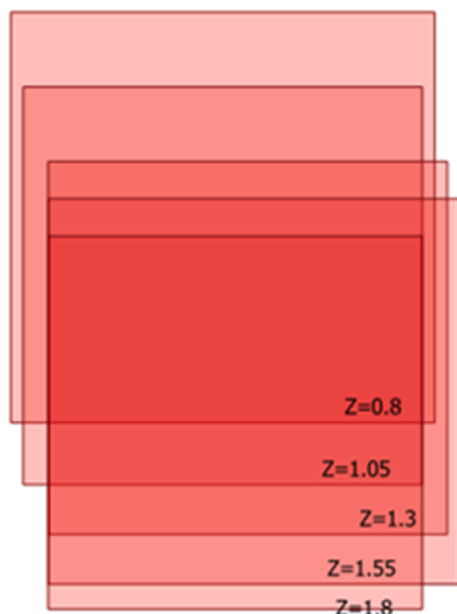


Fig. 4. Example of the detected sections of the trees present in a plot.



**Fig. 5.** Detected sections and adjusted rectangles measuring the two opposite diameters of the tree section ( $d_1$  and  $d_2$ ).



**Fig. 6.** Example of five detections (5 matches) along different heights ( $Z$ ) of a possible tree that overlap more than 75% between each one. This example would be detected as a tree if the match restriction imposed was 5 and more than 75% overlapping was selected in the configuration menu.

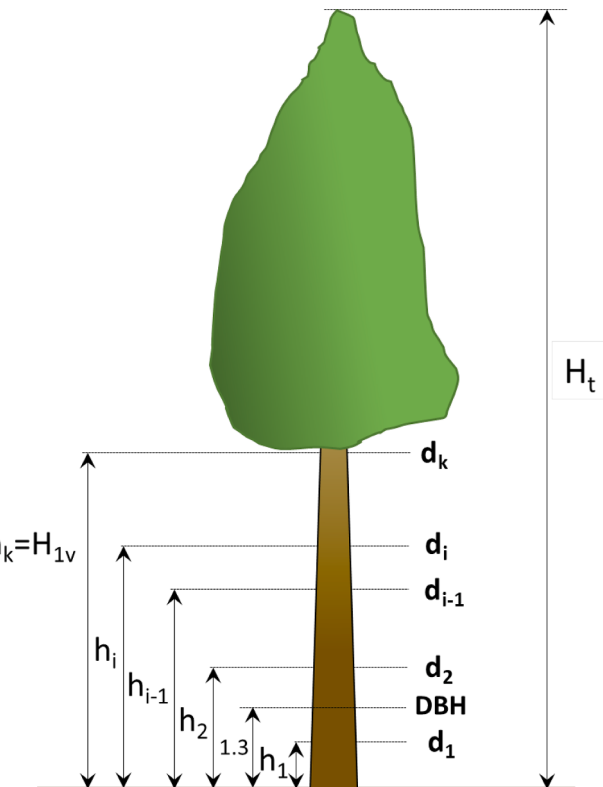


**Fig. 7.** Diameters and heights detected and measured for each tree.

$$ba = \frac{\pi}{4} \left( \frac{DBH}{100} \right)^2$$

$H_t$  (m) is the total height of the tree, calculated from the highest DSM around a planimetric resolution unit relative to the planimetric position of a tree.

$H_{1v}$  (m) corresponds to the height of the highest unit detection in the tree.

According to the Smalian formula (Pardé and Bouchon (1994)),  $V_t$  ( $m^3$ ) is the total volume of the stem, calculated as the sum of all the log volumes (where the log volume is the average section between the top and bottom of the log), multiplied by the log length as follows:

$$V_t = V_1 + \sum_{i=2}^k V_i + V_n$$

where:

$V_1$  is the volume of the first log, i.e., from the ground until the first section detected ( $d_1$ ) at a given height ( $h_1$ ) and is considered a cylinder  $V_1 = \frac{\pi}{4} d_1^2 h_1$ .

$\sum_{i=2}^k V_i$ , is the sum of all the log volumes above the first one until the last detected section ( $k$ ), and  $V_i$  is  $V_i = \frac{\pi}{4} \left( \frac{d_{i-1}^2 + d_i^2}{2} \right) (h_i - h_{i-1})$ , where  $d_i$  and  $d_{i-1}$  are the diameters of the top and bottom sections of the log  $i$ , and  $h_i$  and  $h_{i-1}$  are the heights of both sections respectively.

$V_n$  is the log volume from the last section detected ( $k$ ) to the apex of the tree. Because no intermediate sections are detected, we estimate this volume as a perfect dendrometric shape, calculated using the equation by Pardé and Bouchon (1994):

$$V_n = \frac{\frac{\pi}{4} d_k^2 (H_t - h_k)}{n + 1}$$

where  $d_k$  is the diameter of the highest detected section,  $H_t$  is the total height of the tree,  $h_k$  the height of the section  $k$  (i.e.  $H_{1v}$ ), and  $n$  is a continuous number between 0 and 3, where the value 0 represents a dendrometric shape of cylinder, 1 a paraboloid, 2 a cone, and 3 a neiloid, with the user defining any value within this range.

Of note, because the heights at which a section is obtained are chosen a priori in the configuration menu, when calculating the total volume some sections could find branches, bulges, climbing plants (e.g., ivies), mosses, or lichens. This could cause the sections above the others to have larger diameters, which would be unusual for most tree species. In these cases, the volume obtained through the aforementioned formulae would be an overestimate. Hence, when calculating the volume of each log, AID-FOREST includes the restriction that the upper diameter of a log cannot be larger than the lower diameter. In this case, the upper diameter is ignored, and a new log will be calculated with the next upper section whose diameter is equal or lower than the lower one. The exception to this rule applies to palm species (which are not trees) in which the stems (stipes) may have larger diameters at higher sections, depending on the type of leaf pruning applied. For the sake of practicality, the upper section of a log is considered inadmissible when its diameter is larger than the lower section of the log.

#### 2.1.7. Plot measurement algorithms

At the plot level, AID-FOREST shows the total surface area of the plot based on the size and number of pixels of the DTM (bearing in mind that these plots are clipped in the \*.las files). Because all the detected trees are located at plot level and the tree parameters are measured in each case (see previous step), AID-FOREST sums the additive variables (number of trees, basal area, and volume) or averages the non-additive variables (DBH,  $H_t$ ,  $H_{1v}$ , and dominant height). Finally, it scales the additive plot parameters to the hectare (ha) level, as described in the Appendix.

#### 2.1.8. Compartment or stand calculations

The calculations will differ depending on the kind of inventory

undertaken (sampling or full inventory). In the case of sampling, the plots are distributed within compartments/stands (a compartment is a “canton” in Spanish; the group of cantons make up the so-called “forest”) and then random sampling theory is applied to estimate the average variables at the stand level (per ha), as well as their standard deviations and sampling errors at a 95 % probability level (see the Appendix). If a full inventory is implemented, then only the total variables for the additive variables or average for the non-additive parameters will be calculated. No sampling random error exists because sampling is not conducted.

#### 2.1.9. Crown coverage algorithms for different Z-levels

To compute the crown coverage fraction ( $F_{cc}$ , %) at a specific user-defined height threshold (Z-level; multiple height thresholds can be defined), AID-FOREST obtains one or more raster layers depending on the pre-defined list of crown vegetation coverage thresholds. In this context, pixels with a tree point above the defined threshold (height above ground in the standardised point cloud) are represented in white. Crown coverage is computed as the percentage of white pixels compared to the total number of pixels inside the plot (in the DTM). Because this factor is sensitive to pixel size, AID-FOREST uses the size of the pixel defined by the user in the configuration menu to obtain the DTM. It is advisable to use a small pixel size (e.g., 1–4 cm) to maximise the accuracy of the crown coverage measurements and avoid overestimation of the  $F_{cc}$ .

#### 2.1.10. Outputs and formats

AID-FOREST provides four basic outputs with different formats. The first is an ESRI Shapefile (.shp) format of polygons (rectangles) with the detections at different heights, named ‘boxes.’ These include the ‘ID\_GROUP’ code for trees, height of the sections, score, size of both sides of the rectangle, and number of matches, etc. The second output is an ESRI Shapefile (.shp) format consisting of points, named ‘trees,’ which includes the ‘ID\_TREE’ code, tree positions (x,y), DBH,  $H_t$ , and  $H_{1v}$ ,  $V_t$ , nearest tree number, and distance to the nearest tree (m). The third output is a \*.csv file with the forest stand parameters synthesised at the plot level and also scaled to the hectare level. The fourth output is another.csv file with the forest stand parameters synthesised at the compartment or stand level, including the means, standard deviations, and 95 % probability sampling errors of the different stand variables. In addition, if AID-FOREST is executed in batch mode rather than the user interface mode, standardised point cloud files to the 0 m level, DTMs, DSMs, and DHMs will also be generated.

### 2.2. Light Detection and Ranging (LiDAR) instrumentation and software

In this work, LiDAR data acquisition was conducted using a ZEB-HORIZON (GeoSLAM ltd., Nottingham, UK) as the MTLS device. This consists of a 2D laser range scanner coupled to an inertial measurement unit (IMU) with a motor drive that moves the scanning head to provide the third dimension required to generate 3D information. A novel 3D Simultaneous Localization and Mapping (SLAM) algorithm was used to combine the 2D laser scan data with the IMU data to generate accurate 3D point clouds. The ZEB-HORIZON has as LiDAR device a Velodyne VLP-16 sensor (Velodyne LiDAR, Inc.); this uses an array of 16 infra-red (IR) lasers paired with IR detectors to measure distances to objects. The device is mounted securely within a compact, weather-resistant housing. The array of laser/detector pairs spins rapidly within its fixed housing to scan the surrounding environment, firing each laser approximately 18,000 times per second, providing, in real-time, a rich set of 3D point data. Combining 16 laser/detector pairs into one VLP-16 sensor and pulsing each at 18.08 kHz enables measurements of up to 300,000 data points per second. The laser wavelength is 903 nm, with a 360° × 270° of field of view at a range of 100 m.

The raw data must be processed using the GeoSLAM algorithm via the Geoslam HUB software (supplied with the device) to convert the

encrypted data into a readable format (e.g. \*.las format) which must then be shortened to the desired dimensions (in this case using the Geoslam DRAW GeoSLAM Ltd. software).

Thus, each file contains the plot or stand to be analysed with AID-FOREST. To properly select the offset setting needed by AID-FOREST to process the \*.las files (see Appendix), we measured the DBH of some recognised trees in the field and used Geoslam DRAW to cut slices at 1.3 m above ground. We then assessed the agreement between the DBH measured with this software and the field measurements and used these data to estimate, a priori, a potential offset before processing any data with AID-FOREST.

### 2.3. Experimental design to validate the Artificial Intelligence for Digital FOREST software

To evaluate the accuracy of AID-FOREST to detect and measure trees from a LiDAR point cloud, two specific issues were selected, and the corresponding experimental designs were implemented: (1) to test the ability of the algorithm to detect trees and measure their DBH at plot level; and (2), to evaluate the success of the algorithm in estimating the total stem volume of individual trees. For both objectives, both the classical methodology with callipers and hypsometers (reference method) and the MLTS-AIDFOREST technique were used. This work was carried out in different provinces of Spain (2019–2021) to ensure that AID-FOREST was able to cope with different tree species and stand densities. Table 1 and Fig. 8 show the location of the sites and a summary of their general characteristics.

#### 2.3.1. At plot level

The experimental design used for objective (1) consisted of a nested random design with two factors: (A) tree species and (B) plot size, along with a covariate (C), of tree density, where (C) was nested within factor (B) and both were nested within factor (A). Factor (A), ‘tree species,’

consisted of 5 species; factor (B), ‘plot size,’ ranged from 540 to 34,500 m<sup>2</sup>, and the covariate (C), ranged from 32 to 1,139 trees ha<sup>-1</sup>. Table 1 shows the characteristics of the selected plots and trees. The plots were delimited by poles, including well spheres (one in each corner for small plots), or using the reference point tool in ZEB-HORIZON (which takes a reference point if the device remains static for at least 7 s).

The DBHs of all the trees in the plots were measured using an automatic calliper (Masser BT Calliper, Masser Oy) and a sample of 3–20 trees (depending on the plot size) were selected for total height measurement using a laser hypsometer (TruPulse 200, Laser Technology, Inc.). This work was conducted by two forest technicians. The trees were not positioned at plot level. We also noted the time per plot for field measurements of both the classical and MLTS-AIDFOREST methods, as well as the time required to postprocess point clouds using Geoslam software and AID-FOREST software. The MLTS data acquisition was performed by one technician and consisted of recording a track along the edge and within the plot that started and ended in the same point in order to minimise drift errors during the SLAM. This meant that the distance between the tracks was short (<10 m) for small plots (<700 m<sup>2</sup>). However, for big plots, we increased the distance between the tracks to speed up the field data collection, while always maintaining a distance of less than one third of the maximum allowed by the device (i.e., <33 m).

To check the correlation of the tree detections by AID-FOREST at the plot level, we computed the correctness index (CI) defined as:

$$CI(\%) = 100 \frac{n_z}{n} \quad (1)$$

where n<sub>z</sub> was the number of trees detected by AID-FOREST and n was the real number of trees in the plot. If the CI greater than 100, false trees were detected, while if the CI < 100, some trees were omitted.

To consider the ecosystem visual complexity, which could affect the visibility of the tree stems, and consequently, the point cloud quality, we

**Table 1**

Forest stand characteristics and a description of the sites where the reference (classical forest inventory) and MLTS-AIDFOREST measurements were carried out to evaluate the AID-FOREST performance at plot level and at tree level.

	PLOT SIZE RANGE (m <sup>2</sup> )	# PLOTS	OVERSTOREY SPECIES	UNDERSTOREY SPECIES	TREE DENSITY (trees ha <sup>-1</sup> )	PROVINCE (municipality)	FOREST	†Geographical Coordinates
PLOTS	574–755	16	<i>Pinus halepensis</i>	<i>Ulex parviflorus</i> ; <i>Rosmarinus officinalis</i> ; <i>Thymus</i> sp.	32–773	Valencia (Ayora)	MUP N° 154 “La Hunde y La Palomera”	Lt. 39° 7' 28" Lg. -1° 13' 31"
	577–677	20	<i>P. nigra</i> ssp. <i>salzmannii</i>	<i>Quercus faginea</i> scrubs; <i>Rosa canina</i> ; <i>Berberis hispanica</i>	79–1139	Cuenca (Las Majadas)	MUP N° 133 “Ensanche de Las Majadas”	Lt. 40° 17' 35" Lg. -1° 59' 9"
	540–742	19	<i>P. pinaster</i> ssp. <i>mesogaeensis</i> and <i>Quercus ilex</i> ssp. <i>ballota</i>	<i>Quercus ilex</i> ssp. <i>ballota</i> shrubs; <i>Rosmarinus officinalis</i> ; <i>Thymus</i> sp.	222–672	Cuenca (Almodóvar del Pinar)	MUP N° 166 “Dehesa de Abajo”	Lt. 39° 41' 13" Lg. -1° 51' 19"
	8,410–12,259	6	<i>P. nigra</i> ssp. <i>salzmannii</i>	<i>Quercus faginea</i> scrubs; <i>Rosa canina</i> ; <i>Berberis hispanica</i> ; <i>P. nigra</i> saplings	106–312	Cuenca (Las Majadas)	MUP N° 133 “Ensanche de Las Majadas”	Lt. 40° 15' 40" Lg. -1° 58' 57"
	4,294–7,877	4	<i>P. pinea</i>	<i>Thymus</i> sp.; herbaceous plants	158–223	Albacete (Albacete)	Periurban park “La Pulgosa”	Lt. 38° 57' 46" Lg. -1° 52' 27"
	4,737–4,889	2	<i>P. halepensis</i>	<i>Thymus</i> sp.; <i>Rosa canina</i> ; herbaceous plants	96–112	Cuenca (Cuenca)	Private forest	Lt. 40° 4' 52" Lg. -2° 8' 43"
	4,019–34,467	9	<i>Eucalyptus nitens</i>	<i>Calluna vulgaris</i> , <i>Erica cinerea</i> ; <i>Pteridium aquilinum</i>	215–820	Lugo (Guntín y Palas de Rei)	ENCE forest plantations	Lt. 42° 56' 14" Lg. -13° 41' 50"
TREES	PLOT SIZE (m <sup>2</sup> )	# TREES	OVERSTOREY SPECIES	UNDERSTOREY SPECIES	TREE DENSITY (trees ha <sup>-1</sup> )	PROVINCE (municipality)	FOREST	†Geographical Coordinates
	4,509	37	<i>Fagus sylvatica</i>	<i>Fagus sylvatica</i> saplings; <i>Crataegus monogyna</i> ; <i>Pteridium aquilinum</i>	240	Navarra (Urbasa)	MUP N° 6 “Forest Heritage of the Foral Community of Navarra”	Lt. 42° 50' 14" Lg. -2° 9' 43"
	5,420	34	<i>Quercus rubra</i> ; <i>Q. robur</i> ; <i>Fagus sylvatica</i>	<i>Rubus ulmifolius</i> ; <i>Crataegus monogyna</i>	380	Navarra (Alsasua)	MUP N° 338 “San Pedro y Basabea”	Lt. 42° 54' 28" Lg. -2° 10' 32"

† Lt. Latitude; Lg. Longitude.

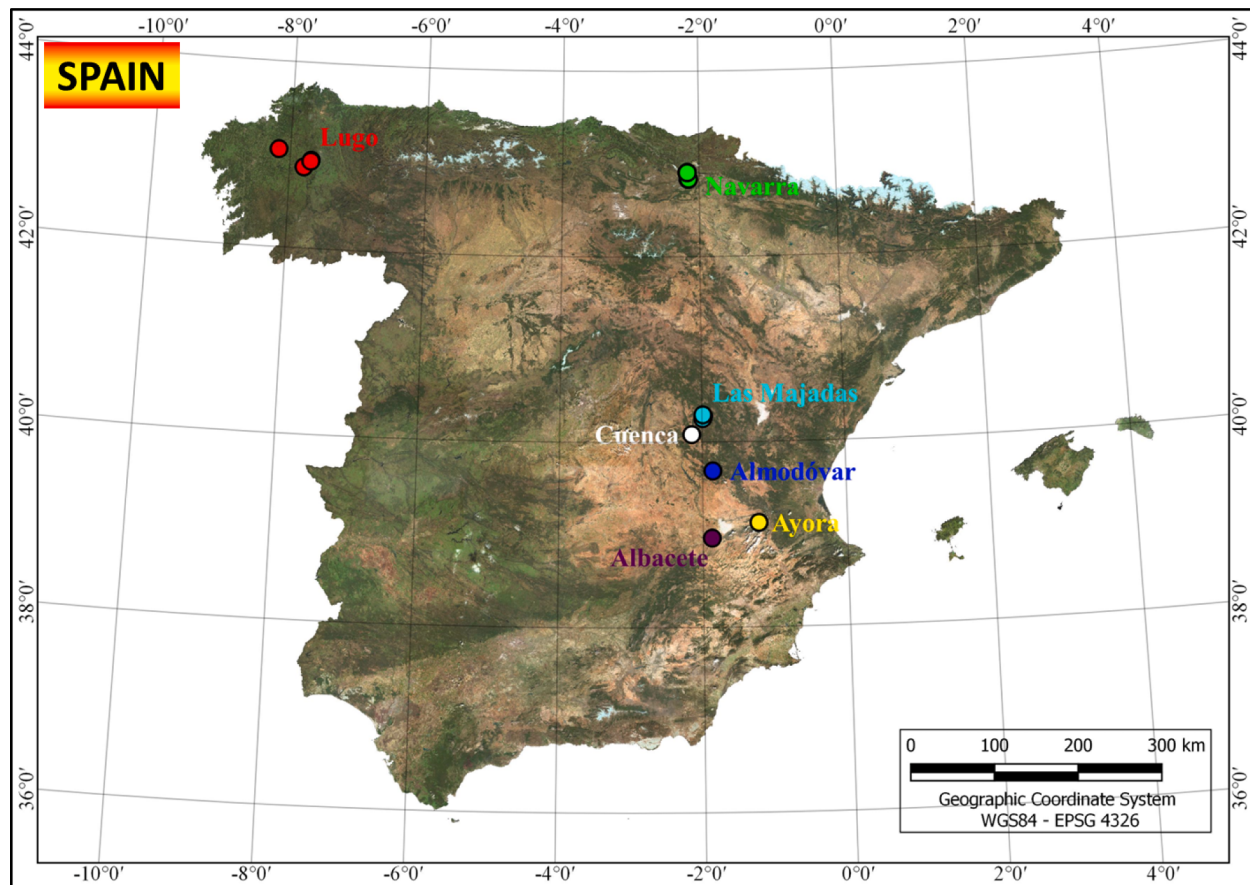


**Fig. 8.** Location of the study sites in Spain. For more details, see Table 1.

created an index called the ecosystem visual complexity index (EVCI). This index is based on the crown coverage fraction of scrub per plot ( $F_{cc_s}$ , %), average height of the scrub ( $H_s$ , m) per plot, and average height of the first verticil of the branches in the tree stems per plot ( $H_{1v}$ , m.). Thus, EVCI is defined by equation (2):

$$EVCI = \frac{F_{cc_s} H_s^3}{H_{1v}^2} \quad (2)$$

For the calculation of EVCI the previously defined parameters were estimated using AID-FOREST twice (except for  $H_{1v}$ , which was obtained directly from AID-FOREST in the first processing) in the following way: The first time, all \*.las files of the plot were processed obtaining, in addition to the tree parameters, the normalised point clouds in \*.las format, which we then shortened by deleting all points above the shrub height using Geoslam DRAW. The second time, the shortened \*.las files (with trees removed) were reprocessed by AID-FOREST to obtain the canopy cover fraction of the shrubs in the following height series: 0.1, 0.3, 0.6, 0.9, 1.2, 1.5, 1.8, 2.1, 2.4, 2.7, and 3 m above ground. Finally, we considered the  $F_{cc_s}$  variable that at 0.1 m above ground and, the average height of the scrub at plot level ( $H_s$ ) being the first height of the series for which the crown coverage fraction was equal or <50 % of the  $F_{cc_s}$  levels.

### 2.3.2. At tree level

To evaluate the AID-FOREST software at tree level, the accuracy of the estimates of the total stem volume (in addition to DBH and total height) of individual trees was tested. In this case, the experimental design consisted of the selection of two different forest stands (Table 1) for which harvesting was planned. Thirty-four to thirty-seven trees of different sizes per site were marked and scanned with the ZEB-HORIZON device (Geoslam ltd.), as described in section 2.3.1, centring the target

tree plot in the centre of a 10 m radius.

Each point cloud was shortened to isolate the objective tree and was then processed using AID-FOREST software. When all the scanned trees were felled and the stems were divided into 1-metre long logs, we measured the diameter of each one (with the bark, top and down) using automatic callipers and calculated the volume using the Smalian formula (Pardé and Bouchon, 1994). Note that *Fagus* and *Quercus* species were usually sympodial and consequently, we quantified the volume of all the branches until the top diameter of the logs was 10 cm.

### 2.4. Statistical analysis

Absolute and relative bias (BIAS, Eq. (3); BIAS (%), Eq. (4), respectively) and absolute and relative Root Mean Square Error (RMSE, Eq. (5) and Eq. (6)) for the DBH and number of trees were calculated considering both the tree and plot as sampling individuals. Because real trees in the plot were not numbered or positioned when classic inventories were carried out, to estimate the BIAS and RMSE of the DBHs at tree level, we sorted the DBHs of both classic and AID-FOREST measurements in descending order, calculating only the outcomes of equations (3), 4, 5, and 6 for the complete cases. However, a pairwise comparison was performed at the tree level in experiment (2) and sorting the trees in descending order was unnecessary.

$$BIAS = \sum_{i=1}^N \frac{(y_i - Y_{zi})}{N} \quad (3)$$

$$BIAS(%) = 100 \frac{BIAS}{\bar{y}} \quad (4)$$

$$RMSES = \sqrt{\sum_{i=1}^N \frac{(y_i - y_{zi})}{N}} \quad (5)$$

$$RMSE(\%) = 100 \frac{RMSE}{\bar{y}} \quad (6)$$

where  $y_i$  is the variable of interest (at plot or tree level) measured using classic methods,  $y_{zi}$  is the variable estimated by MTLS-AIDFOREST, and  $\bar{y}$  is the average of the variable of interest obtained with classic methods.

A general lineal mixed model was implemented to check for significant differences for CI index, depending on factor levels and covariates as well for differences in the BIAS. Factors such as species and plot size were considered as random. To discriminate among the means, we used the Tukey's honestly significant difference (HSD) test (Neter et al., 1996).

To verify that the mean plot-level values obtained with AID-FOREST were close to the values obtained using the classic technique, we used a simple least squares linear regression method (Neter et al., 1996). The variables at the plot level measured with classical techniques were the variables of interest and the predictive variables were those obtained by MTLS-AIDFOREST method. If the model constant was not significantly different from 0 and the slope was not significantly different from 1, we concluded that the variables obtained by MTLS-AIDFOREST accurately estimated the variables obtained by the classic techniques. Student *t*-tests were used to verify that the constant was statistically equal to 0. To verify that the slope did not differ from 1, we analysed it through the confidence interval of the slope, i.e., the mean  $\pm$  the Student *t*-test result  $\times$  the standard error, where the interval had to include 1 for the initial hypothesis to be accepted.

To compare whether the diameter distributions obtained using both techniques were statistically similar, and given that the inventory of plots had not been carried out with numbered trees (i.e. they were not paired samples), we used the comparison of means, medians, and variances of independent samples for each inventory methodology, employing Student *t*-test, F-Snedecor test, and Mann–Whitney U (Wilcoxon) W-test, respectively. Similarly, we used the Kolmogorov–Smirnov test (K–S test) to compare whether the cumulative diameter distributions of both inventory methodologies differed statistically from each other (Neter et al., 1996).

In the case of the volume, DBH, and total height of the individual

trees, where each of them was identified in both methodologies, we used the paired samples technique for comparison (Neter et al., 1996), to evaluate whether the tree-to-tree difference in the parameters (DBH, Ht, and Vt) measured with both techniques significantly differed from zero by applying a Student *t*-test. In addition, to check if the variances and distribution functions were similar, F-Snedecor and K–S tests were used. Furthermore, we conducted multiple regression analysis between the same tree variable obtained with the two different approaches, including dummy variables (species) to check for significant effects on the intercept and slopes of the relationship. All the statistical analyses were performed with Statgraphics Centurion XVI software (StatPoint Technologies, Inc., Virginia, USA).

### 3. Results

#### 3.1. AID-FOREST capability for tree detection and estimation of forest stand variables

The main results of the AID-FOREST evaluation for tree detection are summarised in Table 2. It presents the list of sites and species of the experimental design indicating the number of plots measured with similar surface area and labelled with a corresponding assigned plot size code, as detailed in the bottom of Table 2. In addition, two parameters of the AID-FOREST configuration used in the processing of these plots (i.e. the number of matches and the offset) are listed in the table, as well as the average ecosystem visual complexity index, EVCI, of each set of plots of equal site/species and plot size code. Finally, the tree detection capacity of AID-FOREST is given by the correctness index, (CI, %) or percentage of trees detected, which averaged 96.9 % and ranged from 81.3 to 100 %.

The sites where AID-FOREST showed the poorest detection were Almodóvar del Pinar (*Pinus pinaster*), with a mean CI% of 95.9 % (ranging from 83.3 to 100 %) and Las Majadas (*P. nigra*, plot code 1), with a mean CI% of 96.1 % (ranging from 81.3 to 100 %). In the rest of the sites, the mean CI% exceeded 97 %, with a minimum of at least 90 % (Table 2). To identify the factors that may affect AID-FOREST's ability to detect trees, an ANOVA analysis was performed. Factors such as the species, within-species nested plot size, and number of trees per hectare (D), did not significantly affect the detectability (Table 3). However, EVCI did affect detectability (Table 3), so that the higher the EVCI, the lower the detection rate.

A total of 11,035 trees were measured using the classic forest

**Table 2**

Summary of the sites and species and plot code size of the measured plots to assess AID-FOREST capability for tree detection and estimation of forest stand variables. Values of the setup parameters 'number of matches' and 'offset' used with AID-FOREST are indicated. The average areas and ecosystem visual complexity index (EVCI; including the variables used to calculate it: average crown coverage as a fraction of the scrubs [Fccs]; average scrub height [Hs]; and average height of the first vertical of the trees [H1v]) are listed, as well as, the average, maximum, and minimum values of the correctness index (CI, %).

SITE/SP†	PLOT SIZE CODE‡†	NUMBER OF PLOTS	AREA (m <sup>2</sup> )	MATCH	OFFSET (m)	Fccs (%)	Hs (m)	H1v (m)	EVCI	mean CI (%)	max CI (%)	min CI (%)
Albacete/Pp	2	2	4972	5	-0.075	5.7	0.3	3.1	0.02	96	100	92.1
Albacete/Pp	3	2	7564	5	-0.075	2.2	0.3	3.2	0.01	99	100	98.6
Almodóvar/ Ppr	1	19	643	2	-0.07	34.6	0.4	7.0	0.11	95.9	100.0	83.3
Ayora/Ph	1	16	654	3	-0.05	34.9	0.5	5.9	0.19	97.0	100.0	90.0
Cuenca/Ph	2	2	4813	5	-0.06	24.4	0.3	4.0	0.04	100.0	100.0	100.0
Las Majadas/ Pn	1	20	626	3	-0.06	22.2	0.5	9.6	0.15	96.1	100.0	81.3
Las Majadas/ Pn	3	1	8410	5	-0.08	26.8	0.6	11.5	0.04	98.9	98.9	98.9
Las Majadas/ Pn	4	5	10,817	5	-0.08	37.3	0.6	9.8	0.10	99.4	100.0	98.3
Lugo/En	2	3	4347	3	-0.08	49.8	0.8	13.8	0.14	96.7	100.0	93.7
Lugo/En	3	2	7981	3	-0.08	54.7	0.6	11.9	0.08	97.9	98.6	97.2
Lugo/En	5	4	20,966	3	-0.08	51.6	0.8	14.3	0.13	98.5	99.5	97.3
TOTAL/AVERAGE		76	3227		-0.065	31.6	0.5	8.2	0.13	96.9	100.0	81.3

† SP = tree species: En, *Eucaliptus nitens*; Ph, *Pinus halepensis*; Pn, *Pinus nigra* ssp. *salzmannii*; Pp, *Pinus pinea*; Ppr, *Pinus pinaster* ssp. *mesogeensis*.

‡ PLOT SIZE CODE, 1: < 700 m<sup>2</sup>; 2: 4,019–5,650 m<sup>2</sup>; 3: 7,251–8,410 m<sup>2</sup>; 4: 9,869–11,811 m<sup>2</sup>; 5: 12,259–34,467 m<sup>2</sup>.

**Table 3**

ANOVA analysis of the full regression model for the correctness index (CI, %), depending on factors [species and plot size, nested within the species, SP(AREA)], covariate tree density (D, trees per ha), and ecosystem visual complexity index (EVCI).

	<i>Sum of the Squares</i>	<i>Df</i>	<i>Mean Square</i>	<i>F-Snedecor</i>	<i>Sig. Level</i>	<i>R</i> <sup>2</sup>	<i>SEE</i> <sup>†</sup>
Model	1,006.3	6	167.7	12.65	< 0.0000	48.2	3.6
Residual	914.9	69	13.3				
Total (Corrected)	1,921.2	75					
<b>FACTORS</b>	<b><i>Sum of squares</i></b>	<b><i>Df</i></b>	<b><i>Mean Square</i></b>	<b><i>F-Snedecor</i></b>	<b><i>Sig. Level</i></b>		
SP(AREA)	97.6	4	24.4	1.84	0.1312		
D	34.9	1	34.9	2.34	0.1337		
EVCI	973.5	1	973.5	71.72	< 0.0000		
residual	914.9	69	13.3				
Total (Corrected)	1,921.2	75					

† Standard error of the estimation (SEE), i.e., residual deviation.

inventory method (reference method) in the 76 plots, with their minimum diameter being 2 cm. In turn, AID-FOREST detected 10,712 trees, with the minimum diameter being 8 cm (results not shown). We defined major trees as those measuring at least 11.5 cm (marketable trees in Spain usually measure at least 12.5 cm). Moreover, trees measuring <11.5 cm represented only 1.32 % (149 trees) and 1.19 % (129 trees), respectively in the classic and MTLS-AIDFOREST inventories. Thus, all our subsequent data analyses were conducted considering only major trees.

Tables 4 and 5 show the mean values of detected major trees per plot and of DBH per plot obtained by both techniques for each site/species and plot size, respectively. The BIAS and RMSE of the number of detected trees (# TREESz/PLOT) versus the measured trees (# TREES/PLOT) are shown in Table 4. In general, MTLS-AIDFOREST method underestimated the number of trees per plot by an average of 2.8 % while the relative RMSE was 9.2 %. Besides, the BIAS did not show significant differences either by site/species or by plot size. The poorest results were obtained for the Almodóvar del Pinar and Ayora sites. The BIAS and RMSE of the average DBH estimated by MTLS-AIDFOREST (DBHz) versus the measured (DBH) per plot are shown in Table 5. MTLS-AIDFOREST underestimated the DBH, with the average BIAS for pooled data being 1.8 % and an average RSME of 7.5 %. Again, the BIAS did not show significant differences either by site/species or by plot size, and the same was observed for the RMSE.

Regression analysis between stand parameters at plot level obtained with the classical inventories and with the MTLS-AIDFOREST technique was used to check that the MTLS-AIDFOREST estimates were not statistically unbiased. Table 6 reports the regression coefficients and statistics for goodness of fit between the average diameters at breast height (DBH) obtained for classical inventories (DBH) and MTLS-AIDFOREST estimations (DBHz); and of the linear relationship between the average number of trees per plot obtained for classical inventories (#TREES/PLOT) and MTLS-AIDFOREST estimations (#TREESz/PLOT).

As shown, the two simple linear models were highly significant, and their constants did not differ significantly from 0 and their slopes from 1. Therefore, we can say that MTLS-AIDFOREST adequately estimated the number of trees and average DBH per plot compared to the classic inventory technique, with a residual deviation of 1.12 cm (3.7 % with respect to the average DBH) and 6.4 trees (4.5 % with respect to the mean number of trees per plot), respectively.

We compared the pooled data (DBH and DBHz) of the major trees on the 76 sampled plots by applying a two-sample comparison of independent samples. This analysis showed that there were no significant differences between the means and medians of the distributions of DBH or DBHz (Table 7). Student t-tests were performed to compare the means, assuming that the variances were not equal. The F-test was significant, i.e., there was a statistically significant difference between the standard deviations of the two samples at the 95.0 % confidence level. Finally, the K-S test, which computes the maximum distance between the cumulative distributions of the two samples, showed that there was no statistically significant difference between the two distributions at the 95.0 % confidence level (Table 7). Fig. 9 provides the visual comparison of the histograms of the DBH distributions for the total number of major trees in the 76 plots, obtained by both methodologies (DBH for the classical inventory and DBHz for the MTLS-AIDFOREST system, in cm).

### 3.2. AID-FOREST's ability to estimate DBH, total height and volume at individual tree level

To quantify AID-FOREST's ability to estimate DBH, total Height and total Volume at individual tree, regression analysis was used between each of these tree-level parameters obtained with the classical inventories and those obtained with the MTLS-AIDFOREST technique. The main results of this analysis are summarised in Table 8 (full models). The tree species (*Q. rubra* and *F. sylvatica*) factor did not significantly affect

**Table 4**

Results of the mean number of trees per plot detected by MTLS-AIDFOREST (#TREESz/PLOT) versus those measured by the classical method (#TREES/PLOT). Absolute and relative BIAS and root mean square error (RMSE) are included for each site/species and plot size and for pooled data. Equal letters in the column for relative BIAS (%) and for the site or plot size means there were no significant differences at a 95% probability (Tukey honestly significant difference test). The acronyms used for the plot size and species are as shown in Table 2.

SITE (Sp)	# PLOTS	# TREES/PLOT	# TREESz/PLOT	BIAS(trees)	BIAS (%)	RMSE(trees)	RMSE (%)
Albacete (Pp)	4	115	113	2.25	2.0a	4.50	3.9
Almodóvar (Ppr)	19	22	21	0.53	2.4a	2.51	11.4
Ayora (Ph)	16	24	23	0.94	4.0a	1.60	6.8
Cuenca (Ph)	2	50	50	0.00	0.0a	2.00	4.0
Las Majadas (Pn)	26	57	57	0.69	1.2a	1.52	2.6
Lugo (En)	9	894	866	27.67	3.1a	37.89	4.2
<b>PLOT SIZE</b>	<b># PLOTS</b>	<b># TREES/PLOT</b>	<b># TREESz/PLOT</b>	<b>BIAS(trees)</b>	<b>BIAS (%)</b>	<b>RMSE(trees)</b>	<b>RMSE (%)</b>
1	55	20	20	0.64	3.1a	1.92	9.4
2	7	162	155	6.14	3.8a	10.13	6.3
3	5	217	213	3.40	1.6a	5.23	2.4
4	5	215	213	1.40	0.7a	1.84	0.9
5	4	1,618	1,569	49.75	3.1a	55.12	3.4
<b>ALL SIZES AND SITES</b>	<b>76</b>	<b>143</b>	<b>139</b>	<b>3.96</b>	<b>2.8</b>	<b>13.19</b>	<b>9.2</b>

**Table 5**

Results of the average diameter at breast height at each plot detected by MTLS-AIDFOREST (DBHz, cm) versus those measured by the classical method (DBH, cm). Absolute and relative BIAS and root mean square error (RMSE) are included for each site/species and plot size and for pooled data. Results are shown using the plot as the sampling unit. Equal letters in the column for relative BIAS (%) and for the site or plot size means that there were no significant differences at a 95% probability (Tukey honestly significant difference test). The acronyms used for the plot size and species (SP) are as shown in Table 2.

SITE (SP)	# PLOTS	DBH (cm)	DBHz (cm)	BIAS (cm)	BIAS (%)	RMSE (cm)	RMSE (%)
Albacete (Pp)	4	24.5	24.6	-0.1	-0.5a	0.6	2.4
Almodóvar (Ppr)	19	29.3	28.1	1.2	4.1a	2.4	8.1
Ayora (Ph)	16	28.6	27.7	0.9	3.1a	3.6	12.7
Cuenca (Ph)	2	33.2	33.8	-0.6	-1.8a	0.6	1.9
Las Majadas (Pn)	26	32.9	32.7	0.2	0.7a	1.6	4.9
Lugo (En)	9	28.5	28.4	0.1	0.4a	0.4	1.5
PLOT SIZE	# PLOTS	DBH (cm)	DBHz (cm)	BIAS (cm)	BIAS (%)	RMSE (cm)	RMSE (%)
1	55	30.4	29.6	0.8	2.5a	2.6	8.7
2	7	29.0	29.4	-0.4	-1.3a	0.6	2.0
3	5	28.9	28.4	0.6	1.9a	0.8	2.8
4	5	32.2	32.2	-0.1	-0.2a	0.5	1.5
5	4	27.8	27.6	0.2	0.8a	0.5	1.8
ALL SIZES AND SITES	76	30.2	29.6	0.6	1.8	2.3	7.5

**Table 6**

Regression coefficients and statistics for goodness of fit between (i) the average diameters at breast height (DBH) at plot level obtained for classical inventories (DBH, cm) and MTLS-AIDFOREST estimations (DBHz, cm); and (ii) between the average number of trees per plot obtained for classical inventories (# TREES/PLOT) and MTLS-AIDFOREST estimations (# TREESz/PLOT);  $n = 76$  plots.

	a <sub>0</sub>		a <sub>1</sub>		F-Snedecor	R <sup>2</sup> (%)	SEE	Sig. Level
	M	SE	M	SE				
(i) DBH = a <sub>0</sub> + a <sub>1</sub> DBHz	0.317 <sup>†</sup>	0.809	0.998 <sup>††</sup>	0.027	1386	94.9	1.12	0.000
(ii) # TREES/PLOT = a <sub>0</sub> + a <sub>1</sub> # TREESz/PLOT	0.293 <sup>†</sup>	0.780	1.022 <sup>††</sup>	0.019	284,553	99.9	6.38	0.000

† Constant of the model ( $a_0$ ) which did not differ significantly from 0 at a 95% probability (Student  $t$ -test).

†† Slope of the model ( $a_1$ ) which did not differ significantly from 1 at a 95% probability (confidence interval).

M: mean of the coefficient; SE: standard error of the coefficient; SEE: standard error of the estimation, i.e., the residual deviation.

**Table 7**

Descriptive statistics of the a two-sample comparison of independent samples composed of (i) DBH measured by classical techniques (callipers, DBH) and (ii) DBH estimated by MTLS-AIDFOREST (DBHz), from all trees of the 76 inventoried plots. In addition, some statistical tests for independent samples were performed (Student  $t$ , F, W, and K-S test). Note that the results correspond to the major trees (DBH and DBHz  $\geq 11.5$  cm).

	DBH (cm)	DBHz (cm)
# total of trees	10,887	10,585
Average	28.5	28.3
Standard deviation	10.0	9.8
Standard error	0.1	0.1
Coefficient of variation	35.2 %	34.7 %
Minimum	11.5	11.6
Maximum	91.2	82.6
Stnd. skewness	41.8	37.0
Stnd. kurtosis	37.3	28.5
Student $t$ -test	1.28	0.199
F-test	1.04	0.027
W-test	$5.7 \times 10^7$	0.611
K-S test	1.26	0.084

the variables measured (no significant effects on intercepts or slopes of the model were detected), except for the intercept for both species in the Ht variable (Table 9, simplified models). Although the relationships were good for DBH and Vt ( $R^2 = 97.8\%$  and  $R^2 = 76.1\%$ , respectively; Table 8), the results for Ht were unexpected ( $R^2 = 45.6\%$ , Table 8).

Note that the relationship between the volumes (Fig. 10) showed some anomalous results for five trees (i.e. trees with labels 213, 219, 356, 417, and 424) as well as a low  $R^2$  (Table 8). All these trees had notable bifurcations (Fig. 11) which AID-FOREST was not designed to cope with since the current version of AID-FOREST was optimized for monopodial stems, as described in section 2.1. Hence, to carry out the simplified regression models we removed these five trees (only for

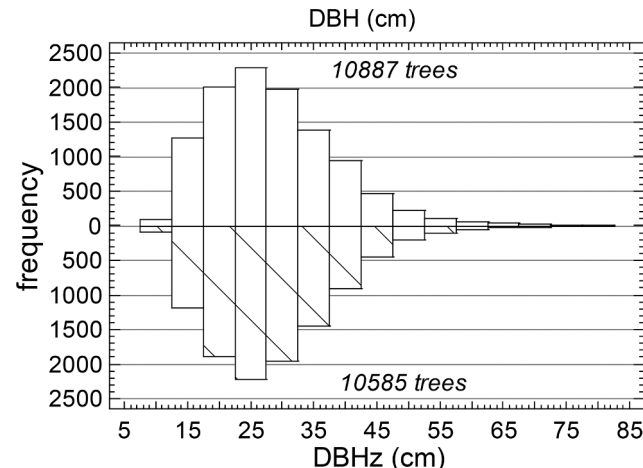


**Fig. 9.** Double histogram showing the diameter distributions of the total number of major trees in the 76 plots, obtained by both methodologies (DBH for the classic inventorying and DBHz for the MTLS-AIDFOREST system, in cm). The total number of major trees is also shown.

volume comparisons) and excluded the non-significant species effect on intercepts and slopes (Table 9). Figs. 12, 13, and 14 show the simplified models for DBH, Ht, and Vt, respectively. MTLS-AIDFOREST did adequately estimate tree parameters (except for Ht) because the relationships were significant and both the constants and slopes were not significantly different from 0 and 1, respectively. For the Ht, MTLS-AIDFOREST produced a species dependent bias and high results variability (see the paired comparison for Ht in Table 10).

According to the paired sample comparison (Table 10), there were no significant differences between the means, medians, variances, or distribution functions (t, W, F, and K-S tests) obtained for DBH and Vt by

**Table 8**

Coefficients of the regression of the full models relating the tree parameters obtained by the two different techniques, classic (DBH, cm; Ht, m; and Vt, m<sup>3</sup>) and MTLS-AIDFOREST (DBHz, cm; Htz, m; and Vtz, m<sup>3</sup>) considering the effect of species (*Quercus rubra* and *Fagus sylvatica*) on the intercept and slope, as well as the statistics related to the goodness of fit.

$DBH = a_0 + a_1 DBHz + a_2 (SP = Q. rubra) + a_3 DBHz (SP = Q. rubra)$				
Parameter	Estimate	Standard Error	t-Student	Sig. Level
a <sub>0</sub>	2.11	1.52	1.39	0.168
a <sub>1</sub>	0.96	0.02	39.4	0.000
a <sub>2</sub>	4.18	2.54	1.65	0.104
a <sub>3</sub>	-0.10	0.06	-1.73	0.089
FULL MODEL	R <sup>2</sup>	SEE	F-Snedecor	Sig. Level
n = 71	97.8	2.4	973.5	0.000

$Ht = a_0 + a_1 Htz + a_2 (SP = Q. rubra) + a_3 Htz (SP = Q. rubra)$				
Parameter	Estimate	Standard Error	Student t	Sig. Level
a <sub>0</sub>	3.07	4.20	0.73	0.467
a <sub>1</sub>	0.88	0.15	5.78	0.000
a <sub>2</sub>	-1.70	7.60	-0.22	0.824
a <sub>3</sub>	-0.01	0.28	-0.05	0.956
FULL MODEL	R <sup>2</sup>	SEE	F-Snedecor	Sig. Level
n = 71	45.6	2.5	20.52	0.000

$Vt = a_0 + a_1 Vtz + a_2 (SP = Q. rubra) + a_3 Vtz (SP = Q. rubra)$				
Parameter	Estimate	Standard Error	Student t	Sig. Level
a <sub>0</sub>	0.16	0.41	0.38	0.703
a <sub>1</sub>	1.05	0.10	10.55	0.000
a <sub>2</sub>	-0.12	0.64	-0.19	0.850
a <sub>3</sub>	-0.04	0.30	-0.12	0.907
FULL MODEL	R <sup>2</sup>	SEE	F-Snedecor	Sig. Level
n = 71	76.1	1.0	72.15	0.000

**Table 9**

Coefficients of the regression of the simplified models relating the tree parameters obtained by the two different techniques, classic (DBH, cm; Ht, m; and Vt, m<sup>3</sup>) and MTLS-AIDFOREST (DBHz, cm; Htz, m; Vtz, m<sup>3</sup>), and statistics related to the goodness of fit. Note that for the volume analysis, five anomalous trees were removed.

$DBH = a_0 + a_1 DBHz$				
Parameter	Estimate	Standard Error	Student t	Sig. Level
a <sub>0</sub>	3.18	1.94	1.64	0.050
a <sub>1</sub>	0.94	0.03	31.31	0.000
SIMPL. MODEL	R <sup>2</sup>	SEE	F-Snedecor	Sig. Level
n = 71	97.6	2.4	2876.45	< 0.000

$Ht = a_0 + a_1 Htz + a_2 (SP = Q. rubra)$				
Parameter	Estimate	Standard Error	Student t	Sig. Level
a <sub>0</sub>	3.20	3.49	0.92	0.363
a <sub>1</sub>	0.87	0.13	6.93	0.000
a <sub>2</sub>	-2.12	0.60	-3.53	0.001
SIMPL. MODEL	R <sup>2</sup>	SEE	F-Snedecor	Sig. Level
n = 71	46.3	2.5	31.24	< 0.000

$Vt = a_0 + a_1 Vtz$				
Parameter	Estimate	Standard Error	Student t	Sig. Level
a <sub>0</sub>	0.02	0.10	0.17	0.864
a <sub>1</sub>	0.98	0.03	31.84	0.000
SIMPL. MODEL	R <sup>2</sup>	SEE	F-Snedecor	Sig. Level
n = 66	94.0	0.42	1013.61	< 0.000

either technique. In other words, the BIAS was not significantly different to 0. However, the opposite was true for Ht because the means, medians, variances, and distribution function were not statistically similar between the two different methodologies used (Table 10). Thus, although not significantly different from 0, MTLS-AIDFOREST underestimated DBH by 0.16 % and overestimated Vt by 1.37 % while the relative RSME (%) was 5.2 % and 14.3 % for these two parameters, respectively. In turn, for Ht, MTLS-AIDFOREST overestimated the total height of the

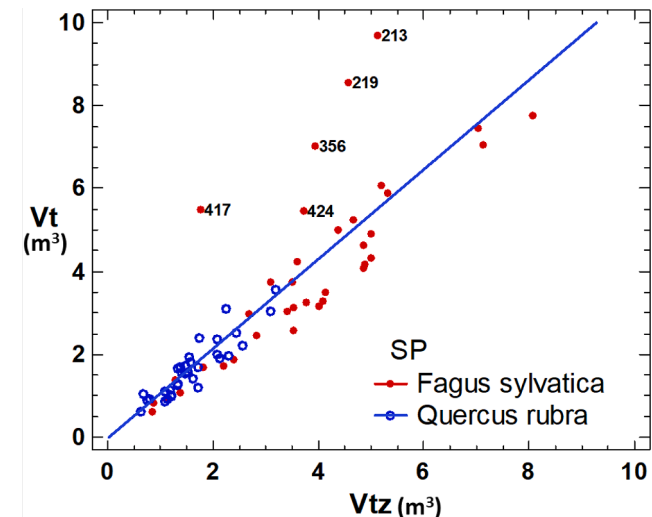


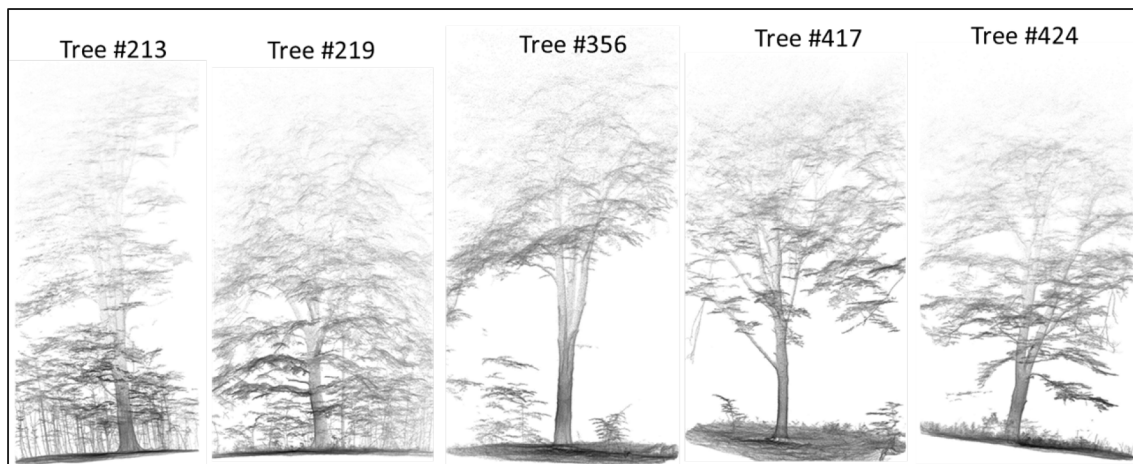
Fig. 10. The relationship between the total tree volume accurately measured by classic methods (V<sub>t</sub>, m<sup>3</sup>) and the total tree volume estimated by the MTLS-AIDFOREST system (V<sub>tz</sub>, m<sup>3</sup>); n = 71 trees (37 *Fagus sylvatica* and 34 *Quercus rubra*).

trees by an average of 1.33 m (5.1 %), with a relative RMSE of 11.5 % (Table 10).

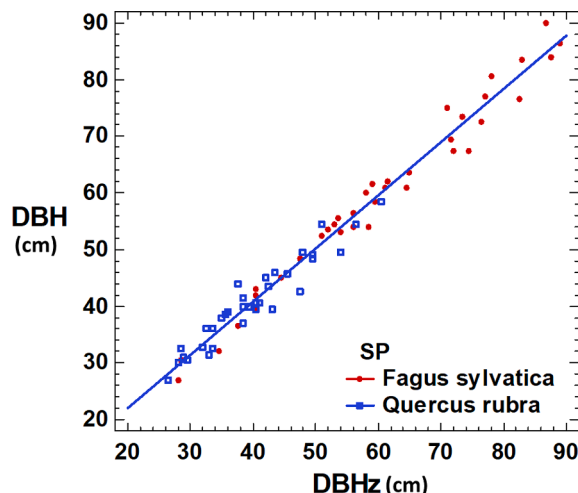
### 3.3. Time required for forest inventorying using both methodological approaches (classic and MTLS-AIDFOREST)

Table 11 shows a summary of the time required for the two different inventory modalities and subsequent data processing for each site and plot size code. On average, 7.2 min was spent on plot-field MTLS scanning using ZEB-HORIZON, versus 81.3 min for classical inventories, thereby representing only 8.9 % of the time spent on classical plot inventorying (R1, Table 11). The processing of raw data from ZEB-HORIZON using Geoslam HUB and DRAW required an additional 18.1 min on average; however, this processing was semi-automatic and does not require complete human control. Finally, an average of 21.3 min was spent processing the \*.las files (each one representing a different plot) using AID-FOREST. However, it is important to remember that this task is fully automated and so the presence of a technician is not required. Thus, the mean overall time invested in completing the MTLS-AIDFOREST methodology to make full forest inventories was 46.6 min and means that completing the full MTLS-AIDFOREST inventory required 57.3 % (R2, Table 11) of the time required to perform classical plot forest inventories (excluding the data postprocessing time in the latter case).

Table 11 also shows the average overall time required for inventorying per hectare. Thus, a classical field forest inventory required 252 min/ha<sup>-1</sup> to measure all the DBHs and a small subsample of total tree height measurements (excluding data postprocessing), compared to the full MTLS-AIDFOREST methodology that required 145 min/ha<sup>-1</sup>, of which 22 min/ha<sup>-1</sup> (15 %) were dedicated to field measurements (handheld scanning by a technician), 66 min/ha<sup>-1</sup> (46 %) to AID-FOREST \*.las file processing (a fully automated task), and 57 min/ha<sup>-1</sup> (39 %) to Geoslam Hub-Draw raw data processing (a semiautomatic task; some data not shown but calculable based on the data shown in Table 11). Finally, Table 12 shows that, as expected, the time invested in field data collection using the classical methodology depended on both the plot size and tree density (the coefficients were all significant at  $\alpha = 0.05$ ). However, data collection by scanning with MTLS depended only upon the plot size (the a<sub>2</sub> coefficient was insignificant).



**Fig. 11.** Five trees (all *Fagus sylvatica*) with notable bifurcations (sympodial stems) that were discarded from the comparison of volumes using both methodological approaches.



**Fig. 12.** The relationship between the DBH (cm) of the tree measured by classic methods and the DBH estimated by MTL5-AIDFOREST (DBHz, cm); n = 71 trees (37 *Fagus sylvatica* and 34 *Quercus rubra*).

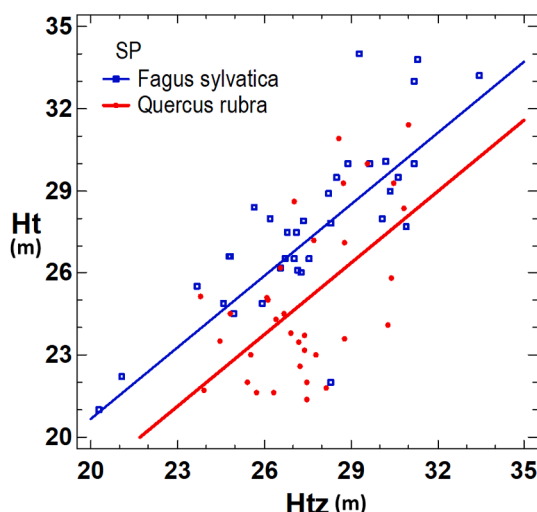


**Fig. 13.** The relationship between the total height of the trees measured by classic methods ( $H_t$ , m) and the height estimated by MTL5-AIDFOREST ( $H_{tz}$ , m) for two tree species; n = 71 trees (37 *Fagus sylvatica* and 34 *Quercus rubra*).

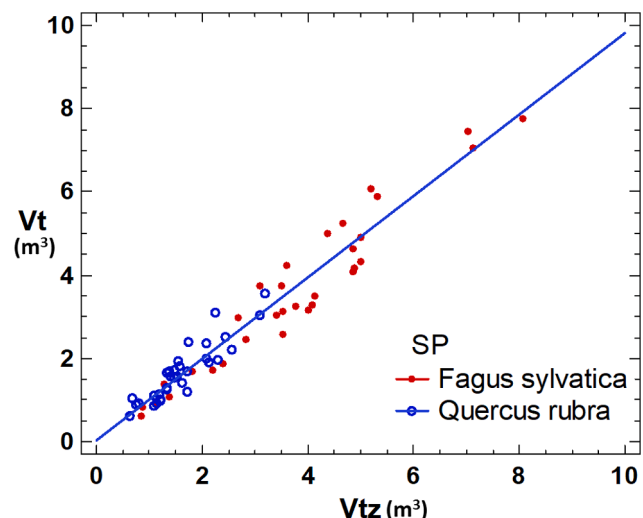


**Fig. 14.** The relationship between the total volume of the tree measured by classic methods ( $V_t$ , m<sup>3</sup>) and the total volume estimated by MTL5-AIDFOREST ( $V_{tz}$ , m<sup>3</sup>) for two species; n = 66 trees (32 *Fagus sylvatica* and 34 *Quercus rubra*). Note that 5 beech trees were removed from this analysis.

#### 4. Discussion

##### 4.1. Detectability and estimation of forest stand variables (Number of trees and DBH) at the plot level

The mean detection rate by AID-FOREST was approximately 97 % and ranged between 81.3 and 100 %. This high success level is at least as good as those reported elsewhere and importantly, was obtained in a fully automated way. For instance, Pfeifer and Winterhalder (2004) obtained poor results by modelling transversal tree sections using free-form curves, with a tree detection rate of 22 to 52 %, depending on whether multiple scans were conducted. This may have been because the point cloud data were from a terrestrial (fixed) rather than a mobile laser.

In contrast, similar to our findings, Bienert et al. (2007) used mathematical morphology techniques to obtain a tree detection accuracy of 97.4 %. In turn, Othmani et al. (2011) employed open-source, semi-automatic Computree software to obtain an average detection rate of 90.6 %. Olofsson et al. (2014) obtained <87 % detectability by using random sample consensus (RANSAC) software with the Hough

**Table 10**

Results and statistics for the paired comparison between the tree parameters obtained by the two different techniques, classic (DBH, cm; H<sub>t</sub>, m; and V<sub>t</sub>, m<sup>3</sup>) and MTLS-AIDFOREST (DBHz, cm; Htz, m; Vtz, m<sup>3</sup>). In addition, average values for both techniques are shown, including the mean diameters, heights, and volumes, as well as the relative BIAS (%) and absolute and relative RSME.

(DBH – DBHz)	Sig. Level	(Ht – Htz)	Sig. Level	(Vt – Vtz)	Sig. Level
n	71	n	71	n	66
BIAS	0.08	BIAS	-1.33	BIAS	-0.04
BIAS (%)	0.16	BIAS (%)	-5.10	BIAS (%)	-1.37
RMSE	2.63	RMSE	3.01	RMSE	0.42
RMSE (%)	5.2	RMSE (%)	11.51	RMSE (%)	14.33
Std. Dev.	2.64	Std. Dev.	2.72	Std. Dev.	0.42
Std. Skew.	-1.5	Std. Skew.	-1.95	Std. Skew.	0.23
Std. Kurt.	0.06	Std. Kurt.	-0.09	Std. Kurt.	-0.60
t-test	0.26	t-test	-4.13	t-test	0.77
F-test	0.90	F-test	2.06	F-test	1.02
W-test	2481	W-test	3176	W-test	2216
K-S test	0.07	K-S test	1.68	K-S test	0.52
DBH	50.6	Ht	26.1	Vt	2.61
DBHz	50.5	Htz	27.5	Vtz	2.65

**Table 11**

Average time spent (in minutes) measuring the forest stand parameters across the sites and species and by plot size code using the two different techniques: (i) classic measurements carried out by two technicians (one for DBH measurement and another for total height measurements on a sample of 3–20 trees per plot) and (ii) MTLS measurements carried out by one technician. Note that, for the classic inventory, only time spent on field data collection was computed (postprocessing data was not considered). The acronyms used for the plot size codes are as shown in Table 2; n = 76 plots.

SITE	SIZE CODE	# PLOTS	AREA (m <sup>2</sup> )	Density (trees ha <sup>-1</sup> )	T-classic (min)	T-MTLS (min)	R1 %	T-Geoslam (min)	T-AIDF (min)	T-Total (min)	R2 %	T-Classic (min/ha)	T-MTLS (min/ha)	T-Total (min/ha)
Albacete	2	2	4,972	159	88.2	8.7	9.9	21.8	32.8	63.4	71.8	177	18	127
Albacete	3	2	7,564	201	159.0	7.7	4.8	19.1	49.9	76.7	48.2	210	10	101
Almodóvar	1	19	643	379	15.0	3.8	25.5	9.6	4.2	17.6	117.4	233	59	274
Ayora	1	16	654	360	13.4	3.1	22.9	7.6	4.3	15.0	112.3	204	47	230
Cuenca	2	2	4,813	104	25.8	8.4	32.6	16.8	24.1	49.3	191.1	54	17	102
Las Majadas	1	20	626	289	11.4	3.2	28.1	8.0	4.1	15.3	134.6	181	51	244
Las Majadas	3	1	8,410	106	145.8	17.1	11.7	42.8	55.5	115.4	79.1	173	20	137
Las Majadas	4	5	10,817	194	317.5	21.8	6.9	54.6	71.4	147.8	46.5	294	20	137
Lugo	2	3	4,347	682	116.3	7.2	6.2	18.1	28.7	54.0	46.4	268	17	124
Lugo	3	2	7,981	448	145.2	13.9	9.6	34.8	52.7	101.3	69.8	182	17	127
Lugo	5	4	20,966	781	635.2	35.0	5.5	87.4	138.4	260.8	41.1	303	17	124
			3227	353	81.3	7.2	8.9	18.1	21.3	46.6	57.3	252	22	145

T-classic (min): time spent on the classic plot inventory including their setting.

T-MTLS (min): time spent scanning the plot with the ZEB-HORIZON equipment.

T-Geoslam (min): time spent processing the raw data from the MTLS on each plot using Geoslam HUB and DRAW.

T-AIDF (min): time spent processing the \*.las files for each plot using AID-FOREST.

T-Total (min): total time spent per plot to complete the whole MTLS-AIDFOREST inventory, i.e., (T-MTLS) + (T-Geoslam) + (T-AIDFOREST).

R1: ratio of T-MTLS/T-classic (percentage).

R2: ratio of T-Total/T-classic (percentage).

transform when the distance from the sensor was <10 m. Indeed, Bauwens et al. (2016) obtained 100 % detection in small plots ( $\approx 700 \text{ m}^2$ ) when also using Computree software and implementing the algorithms from the ONF-ENSAM plugin (Othmani et al., 2011). Furthermore, Cabo et al. (2018a) developed an automatic method that detected more than 99 % of trees. Hyppä et al. (2020b) also reported a tree detection rate near 100 % and low bias using a novel postprocessing algorithm to extract stem curves from scan-line arcs. Mokroš et al. (2021) used the cylinder-based algorithm for tree detection and measurement and detected 90.6–100 % of the trees. Finally, Vatandaşlar and Zeybek (2021) used machine learning and innovative algorithms for tree detection and measurement to obtain detectability that exceeded 100 % (i.e., there were false detections). Nonetheless, none of these aforementioned works applied their algorithms to large plots and so it is impossible to state their applicability and functionality in these cases.

The basis of AID-FOREST section detectability is the recognition of shapes like the outer ring in each band (Figs. 3 and 5). In addition, tree detectability requires a minimum number of vertical detected sections

(multiple bands) and a minimum defined amount of overlapping. Consequently, success will depend both on the good definition of the outer ring sections and an appropriate number of selected matches. Well-defined outer ring sections depend exclusively on the point cloud quality and the user-defined number of matches depends on species characteristics, mainly the stem length free of branches (or scrub). Point cloud quality (in terms of adequately ‘seeing’ the tree stems) is a function of the distance between scanning paths, presence of high scrub, and tree density of the stand (which could hide the trees, even when using mobile LiDAR). Thus, the number of matches chosen differed according to the species and forest stand characteristics (Table 2).

A low number of matches were selected when the expected probability of section detections was low. This occurred for small plots of *Pinus pinaster* species (in Almodóvar del Pinar) where the understory was dominated by *Quercus ilex* ssp. *ballota* coppices (1–2 m high), and in small plots at the Las Majadas site at which *P. nigra* saplings (over 2–3 m high) were abundant. However, the low number of matches increased the probability of false detections and, on the contrary, the high number

**Table 12**

Regression models relating the time spent on field data collection at the plot level using classical inventories (*T*-classic, minutes) and the MTLS method for scanning plots (*T*-MTLS, minutes), as a function of the PLOT-SIZE ( $m^2$ ) and TREE-DENSITY (trees per hectare of the plot), as well as the statistics related to the goodness of fit.

$T$ -classic = $a_0 + a_1$ PLOT-SIZE + $a_2$ TREE-DENSITY				
Parameter	Estimate	Standard Error	Student t	P-Value
$a_0$	-34.9	7.79	-4.49	0.0000
$a_1$	0.03	0.001	36.98	0.0000
$a_2$	0.07	0.02	3.50	0.0008
FULL MODEL	$R^2$	SEE	F-Snedecor	Sig. Level
n = 76	95.4	36.00	774.3	0.0000

$T$ -MTLS = $a_0 + a_1$ PLOT-SIZE + $a_2$ TREE-DENSITY				
Parameter	Estimate	Standard Error	Student t	P-Value
$a_0$	2.22	0.56	3.95	0.0002
$a_1$	0.0015	0.00006	27.52	0.0000
$a_2$	0.0001	0.0014	0.075	0.9403
FULL MODEL	$R^2$	SEE	F-Snedecor	Sig. Level
n = 76	91.5	2.6	406.1	0.0000

of matches enhanced the probability of no tree detections. According to our results, there were no false detections, but there were no detections. In contrast, the high number of matches was used to guarantee no false detections when the stem length free of branches was high. This occurred in the case of *Pinus pinea* in a peri-urban park (Table 2) in which fountains, woody fences, lamp posts, wood poles, and statues, etc., could be mistakenly identified as trees. Similarly, five matches were used in managed forest stands with long (2–3 m), branch-free stems such as *Pinus halepensis* (Cuenca) or *P. nigra* (Las Majadas).

On the one hand, we processed all the \*.las files from the same site and plot size using the same AID-FOREST settings. However, because the characteristics of some sites differed over the space, the selected number of matches per site was likely not optimal. This could justify the existence of some undetected trees within these plots. On the other hand, no trees with a DBH below 8 cm were detected. This may be because the noise of the point cloud for these thin trees exceeded their radius. Consequently, no outer ring-like shapes were conformed and so the trained model was unable to consider them as tree sections. Therefore, the lack of detections for small trees likely resulted from technological restrictions in the point cloud quality. For comparison, Riddings et al. (2015) found that the minimum detected DBH was 5 cm when using a Zeb-Revo1 (Geoslam) MTLS with manual detection through the Leica Cyclone software. However, they also suggested that removing trees measuring <10 cm from the analysis improved the accuracy of their

results. Similarly, using a ZEB-HORIZON MTLS device, Mokroš et al. (2021) found that the accuracy and detectability improved when only trees measuring more than 10–20 cm were considered in the analyses.

To the best of our knowledge, this is the first time that tree detectability at the plot level can be explained using an objective index, in our case, the EVCI (Tables 2 and 3). In addition, we used our own software to objectively extract the parameters used to calculate the EVCI from the point cloud. Finally, EVCI, but not tree species or tree density, significantly affected the tree detectability (Table 3). This means that AID-FOREST could be universally applicable within the context of the forest parameters detailed in this current work. Indeed, it would be useful to extend this experiment to tree species and forest stands with other characteristics.

Besides of the ‘number of matches,’ another important user-defined parameter within the AID-FOREST settings is ‘offset adjust,’ which is directly related to the accuracy of the DBH estimations. Our results indicate that, in addition to species, the greater the plot area, the higher the offset (Fig. 15). Note that offset is a discount (negative value, m) from the diameter obtained as the average of the two sides of the box. It may seem illogical that the same tree species had different offsets when the selected plots were different sizes (Table 2; *P. nigra* and *P. halepensis*) while other species such as *Eucalyptus nitens* had the same offset for different plot sizes. However, this effect can easily be explained as follows. When all the factors except the species are constant during the scanner tracking, bark rugosity will determine the point cloud noise around the stem. However, if the distance from the scanner to the stem is variable, both the rugosity and distance will drive the point cloud noise (regardless of other external factors such as branching or the presence of scrub).

It appears that this scenario occurred for *P. nigra* and *P. halepensis*, two natural forest stands in which the distance between the stems and scanner for small plots was lower than that for bigger plots. This can be deduced from Table 11, where the scan time (*T*-MTLS) for small plots such as Las Majadas-1 and Ayora-1 were 51 and 47 min/ha<sup>-1</sup>, versus Las Majadas-2 or -3 or Cuenca-2, where 20 and 17 min/ha<sup>-1</sup> were spent scanning. Thus, the scanning had to be carried out on more separated tracks on big plots compared to smaller ones. The opposite occurred for *E. nitens* (Lugo), an artificial forest stand where the trees were spaced out in 3.2 m × 3.2 m squares and the scanner tracking was conducted uniformly along the tracks formed by the trees; in other words, where the distance between the tracks in all the plot sizes remained constant. Similarly, as shown in Table 11, the same amount of time was spent regardless of the plot size in Lugo (17 min/ha<sup>-1</sup>) and consequently, no differences in the offset were required. Ideally, the same criteria would be followed while scanning, independently of the plot size. However,

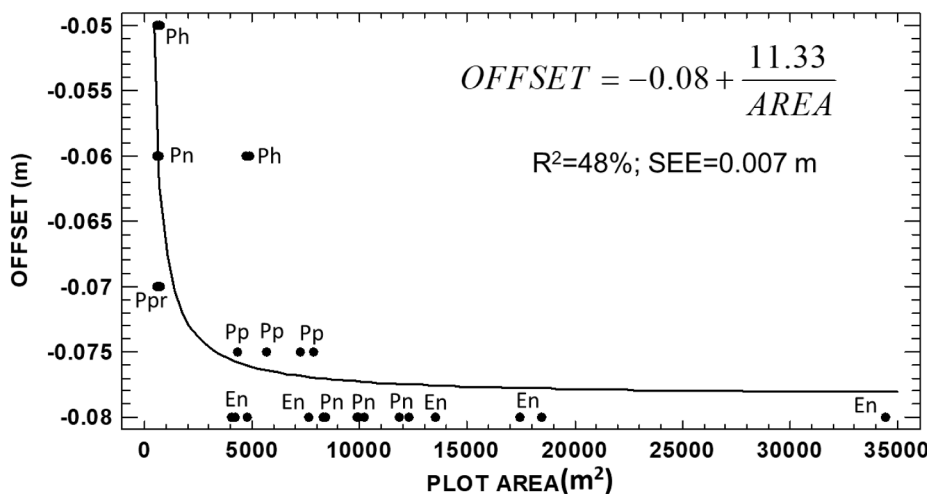


**Fig. 15.** Relationship between the offset (m) and plot size ( $m^2$ ); n = 76 plots. The acronyms used for the species are as shown in Table 2.

this would lead us to exceed the maximum time for scanning data collection (30 min) recommended by the manufacturer of LiDAR (although we have processed data collected over nearly 1 h). Thus, AID-FOREST is equipped with the ‘offset adjust’ parameter to cope with this inconvenience.

For the mean number of trees per plot, we found that the accuracy at plot level was comparable with the findings from other work. Hence, the relative BIAS and RMSE were 2.8 % and 9.2 %, respectively (Table 4). Although there were differences in the BIAS depending on the site, species, and plot size considered, these values were not statistically significant at  $\alpha = 0.05$  (Table 4).

For the mean DBH at plot level, the BIAS and RMSE were 1.8 % and 7.5 %, respectively (Table 5). Similarly, there were no significant differences in these values according to the site, species, or plot size factors (Table 5), although BIAS variability could be explained for the particular offset chosen for each site and plot size, in addition to the particular forest plot characteristics. After applying a Student *t*-test to compare the means (data not shown) we concluded that the BIAS was not significantly different to 0 at the plot level ( $t = 0.28$ ;  $p = 0.78$ ;  $n = 76$ ).

In other work using a ZEB1 MTLS (Geoslam Ltd.), Ryding et al. (2015) reported BIAS of  $-5.6\%$  to  $19.5\%$  and a RSME of 9 % to 46 % for DBH, depending on whether DBH greater than 10 or  $< 10$  cm was selected, respectively. Using a MTLS device and point-cloud processing technique, Liang et al. (2019) reported a relative BIAS and RMSE of 1–15 % and 10–35 %, respectively, depending on the difficulties of the forest. Similarly, using the same MTLS as us (a ZEB-HORIZON) and automatically processing their data with the Ordering Points to Identify the Clustering Structure (OPTICS) algorithm, Gollob et al. (2020) obtained a RMSE between 2.87 cm (14.85 %) and 3.32 cm (17.18 %) and a BIAS of  $-0.48$  cm ( $-2.48\%$ ) to  $0.03$  cm (0.16 %). We did not find any references regarding the plot size effect on BIAS.

#### 4.2. Accuracy to assess individual tree parameters (DBH, Ht, and Vt)

The paired sample comparison at tree level, shown in Table 10, strongly confirmed that AID-FOREST estimated DBH without statistical bias. This was already reported at plot level and widely discussed in section 4.1.

However, our results showed that there was discrepancy between the tree height measured in the field (Ht) and that given by AID-FOREST (Htz), although this disagreement can be easily explained. The total height of the tree was measured up to the apex (10 cm diameter) of the main axis (i.e., the most vertical stem if various stems were present) in the field once the tree was felled. However, AID-FOREST takes the total height as the highest DSM value in an environment of one unit of planimetric resolution of the highest point detected on the tree (see the Appendix for more details). Consequently, AID-FOREST gives the highest height of the tree crown, not that of the stem to the top diameter of 10 cm, because branches and leaves rise above the stem (depending on structural development of the crown of each species; Fig. 13). Nonetheless, very little previous academic work has described how their total heights were measured in the field. In general, most authors indicate that in classic methods the total height is measured using an analogue or digital hypsometer, but none defined with precision the total height measured. Thus, the comparison between methodologies is haphazard and makes it impossible to draw well-founded conclusions.

When a non-mobile TLS is used, the total height is underestimated by the software or algorithm used, mainly because it is unable to ‘see’ the upper level of the trees (occlusion effect). Thus, Liang et al. (2016) reported underestimation of tree height by up to several metres, suggesting that further study is required. Similarly, Cabo et al. (2018b) reported underestimations of the average height at plot level of 3.2 to 18.5 m, depending on the species. Using MTLS, Heo et al. (2019) reported an average underestimation of the total height by 0.24 to 0.4 m. However, on the contrary, using a ZEB1 MTLS (Geoslam, Ltd.) and its accompanying Computree software, Del Perugia et al. (2019) found a

BIAS of only 0.17 m for *Castanea sativa* trees. Employing ZEB-HORIZON (Geoslam, Ltd.) and a custom methodology including RANSAC cylinder fitting, Donager et al. (2021) reported overestimation of the total tree height by about 1.3 m in *Ponderosa pine*, a similar result to our findings (Table 10). In conclusion, AID-FOREST extracted a total height that did not agree conceptually with the total height we defined in our field study work, and in addition, the outcome depended on the tree species because of their different crown shapes (Fig. 13). However, the top height AID-FOREST provides should be adequate when compared to the results from hypsometers because it is practically impossible to aim at the exact portion of the stem with a minimum particular diameter.

For the overall tree stem volume, our results showed that the estimation by AID-FOREST was statistically unbiased (BIAS =  $-0.04 \text{ m}^3$ , equivalent to  $-1.37\%$  of the average volume; Table 10). Although the BIAS was not statistically significantly different to 0, it there was a slight overestimation. However, it seems contradictory, or at least unexpected, that AID-FOREST, which was designed primarily to obtain the volume of monopodial trees, adequately estimates the total volume of sympodial trees. Revisiting the pipe model theory by Shinozaki et al. (1964a, 1964b) could offer a possible explanation for the agreement between the measured volumes and those estimated by AID-FOREST. AID-FOREST computes the stem volume that is within the crown as a pure dendrometric shape; this dendrometric type has a basal section as the latest detected section in the stem (i.e., where the crown starting, at the height H1v), and a height equalling the crown length, i.e., the difference between Ht and H1v (see section 2.1.6 and the Appendix). If bifurcations start within the tree crown length, sections of the multiple stems at any height within the crown could be considered equal to a hypothetic single stem with a section equal to the sum of the multiple cross sections of the stems (Shinozaki et al., 1964a, 1964b). Thus, all the trees included in the AID-FOREST analysis contained bifurcations in the crown length, while the five trees we removed from our analysis (Figs. 10 and 11) had bifurcations below the start of the crown.

In general, most previously published work did not estimate a reference tree or plot volume and focussed exclusively on tree detection and measurement of their diameters and heights. Others compared the volumes obtained from point clouds with a reference volume estimated with local volume tables (Hyppä et al., 2020a; Vatandaşlar and Zeybek, 2020, 2021) or via allometric volume or regional species-specific models. Moreover, very few articles had accurately measured the reference volume by summing the volumes of small logs from felled trees that were divided and measured (Mengesha et al., 2015) or sometimes by using TLS (Bienert et al., 2018; Hyppä et al., 2020a; Liang et al., 2018). Our results were validated using real stem volumes and, consequently, are sufficiently robust to be conclusive, thereby making our results, which were obtained in non-monopodial trees, hopeful and promising. Nevertheless, additional tree species and forest stands should be selected to universally validate our results at the tree level.

Despite the above, the comparisons conducted with accurate volume measurements were poor. Thus, using Autostem<sup>TM</sup> software to process the point cloud, Mengesha et al. (2015) reported a relative BIAS of 11–22 %. In turn, Vatandaşlar and Zeybek (2021) used machine learning (e.g., a Random Forest classifier for tree detection) and innovative algorithms (e.g., ellipse fitting to estimate the diameter of noncircular trees) and reported poor agreement between the estimated and reference volumes (with deviations of up to 21.5 %). This may have been because the reference volume was obtained from allometric estimations rather than accurate volume measurements. Similarly, Hyppä et al. (2020a) used a postprocessing algorithm chain to extract stem curves from scan-line arcs corresponding to individual trees and reported a BIAS of  $-1.5$  to  $-3.8\%$  and relative RMSE of 11.7–26.0 % for timber volume by using Finnish volume tables. Finally, Bienert et al. (2018) used their previously published approach to tree detection (Bienert et al., 2007) and the quantitative structure model (QSM) to measure tree volumes, using the TREEQSM (v.2.30) software developed by Raumonen et al. (2013) for QSM execution. They found that, compared to the

volumes estimated via TLS, the marketable and total volume of the modelled QSM were underestimated by up to 5 m<sup>3</sup> in 500 m<sup>2</sup> plots.

#### 4.3. Time analysis

Very few works provided information about the time invested in carrying out classic field survey inventories compared to mobile (MTLS) or fixed (TLS) laser scanning. Some of them, such as Liang et al. (2014) suggested that a plot of 2,000 m<sup>2</sup> could be scanned in a few minutes by employing a handmade system (built by the Finnish Geodetic Institute and based on FARO Focus 3D software). Others such as Ryding et al. (2015) reported requiring 200 min/ha<sup>-1</sup> per surveyor when a ZEB1 MTLS was used in 100 m<sup>2</sup> plots, compared to 11,765 min/ha<sup>-1</sup> per surveyor using a TLS (FARO Focus 3D), or 23,256 min/ha<sup>-1</sup> per surveyor for a classic field survey. These high times reported for MTLS systems are likely because the old ZEB1 device was used.

However, none of these studies reported the time required for data processing to obtain the relevant dendrometric parameters. Using ZEB-REVO-RT, Chen et al. (2019) reported requiring 10 min per 300 m<sup>2</sup> plot (5 min for surveying, -166 min/ha<sup>-1</sup> and 5 min – 166 min/ha<sup>-1</sup> for processing), in other words, a total time of 333 min/ha<sup>-1</sup> compared to 10,989 min/ha<sup>-1</sup> for classic field surveys. In contrast, Apostol et al. (2018) reported a measurement time of 120 or 15–90 min per 500 m<sup>2</sup> plot for classic and TLS scanners, respectively, depending on whether single or multiple scans were performed, but did not report the corresponding data processing times required. Finally, Bauwens et al. (2016) compared TLS, MTLS, and classic field measurements in circular plots with a radius of 15 m (707 m<sup>2</sup>) and included field work and processing times. They reported 24 min per plot (339 min/ha<sup>-1</sup>) using a ZEB1 MTLS and of 10 min for single (141 min/ha<sup>-1</sup>) or 75 min (1,061 min/ha<sup>-1</sup>) for multiple scans when using a FARO Focus 3D TLS. For classic field measurements a total of 32 min per plot (453 min/ha<sup>-1</sup>) was reported. For data processing they reported 106 min per plot (1,499 min/ha<sup>-1</sup>) for MTLS, 84 min per plot (1,188 min/ha<sup>-1</sup>) for TLS, and 10 min per plot (141 min/ha<sup>-1</sup>) for classic field measurements.

All the above-mentioned survey times were much slower than ours. For MTLS scanning, the reported times ranged between 166 and 339 min/ha<sup>-1</sup> compared to our 22 min/ha<sup>-1</sup> (Table 11). The most likely reason for this difference was the MTLS device used because all the articles we mentioned used the more limited ZEB1 or ZEB-REVO scanners, whereas here we used ZEB-HORIZON. In contrast, Mokroš et al. (2021) reported a total scanning time of 10 min for plots of 625 m<sup>2</sup>, or in other words, 160 min/ha<sup>-1</sup>. Similarly, Gollob et al. (2020) described a total scanning time of 10.96 min for 1,257 m<sup>2</sup> plots (87 min/ha<sup>-1</sup>). Conversely, our results (only 22 min/ha<sup>-1</sup>) were equivalent to approximately 1/7 to 1/4 of these previously reported times. Perhaps this disagreement was because of the different characteristics of the forest stands studied or the different computing time criteria applied. In this sense, we only computed the time required for the scanning but did not include the time spent setting up the plot for measurement.

On average, the processing time required by AID-FOREST was 66 min/ha<sup>-1</sup>. To the best of our knowledge, no previous publications have reported the time required to detect the trees and measure them. Only the work by Bauwens et al. (2016) estimated the “time processing” as 106 min per plot (1,499 min/ha<sup>-1</sup>) but did not clearly state what this processing time included. Regardless, their findings vastly differed from the 66 min/ha<sup>-1</sup> required to process the AID-FOREST \*.las files or the 57 min/ha<sup>-1</sup> needed for Geoslam Hub-Draw raw data pre-processing. Finally, it is worth noting that the aforementioned AID-FOREST data processing time was obtained with a laptop without a graphic card (Intel® Core™ i7-9750H CPU, 2.60 GHz, 32 GB RAM); when a slightly more powerful computer (Intel® Core™ i7-9700 K CPU, 3.60 GHz, 32 GB RAM) with a graphic card (NVIDIA GeForce GTX 1080 Ti) was used, the processing time was reduced from 66 to 29 min/ha<sup>-1</sup> (data not shown). Consequently, the performance of AID-FOREST when processing points clouds strongly depended on the computing power available

and the difficulty in processing the point cloud parameters. In other words, the number of bands (raster) requested (data not shown).

#### 4.4. The software

AID-FOREST stands out for its fundamentals and its ability to process point clouds. Indeed, this is the first time an algorithm based on artificial intelligence has been used to detect tree sections. In addition, unlike the work by Chen et al. (2019), in which the noise had to be eliminated twice from the raw point clouds before they could be processed, no such pre-processing is required by AID-FOREST. Similarly, Liang et al. (2018) also removed noise from the point cloud before data processing. While low levels of data noise improves the detectability and diameter measurements (Chen et al., 2019) its removal also increases the associated processing times and costs. In contrast, some authors performed pre-scan preparation of the forest stands (for example, by pruning or removing scrub) before MTLS scanning, as reviewed by Liang et al. (2016). Obviously, pre-scan treatment improves the detection and measurement of trees because low branches or scrub hiding the stems are removed, thereby improving the point cloud quality. Nonetheless, other work concluded that pre-scan forest preparation did not improve detection (Mengesha et al., 2015), likely because a fixed terrestrial laser scanner was used.

-FOREST is not limited by plot size; as shown in Table 1, we processed plots measuring nearly 3.5 ha. On the contrary, most of the literature we consulted assessed small plots (not exceeding 1,000–2,000 m<sup>2</sup>). AID-FOREST can process hundreds of hectares and is only limited by the restrictions of the MTLS device used. Additionally, processing by AID-FOREST software is fully automatic and does not need human supervision once it has been launched. As stated by Ryding et al. (2015), “An important factor in the development of point cloud data sets for use within forest modelling will be the automation of data processing. Without automation, these very large, complex data sets are too time-consuming to process manually and would not be considered a practical survey solution”. Liang et al. (2016) also noted that no automatic software was available to process forest point cloud data and that when it became available, it would be too expensive. Similarly, Donager et al. (2021) stated that “the lack of tools for easily processing terrestrially-collected lidar datasets in an automated fashion, targeting conservation and management applications, quickly became apparent in our work”. Although AID-FOREST still needs improvement, it comes much closer to solving some of these problems. The cost of AID-FOREST is near € 4,000 for an unlimited license (a free trial can be requested at dielmo@dielmo.com), which is reasonable when compared to the total cost of manually completing forest inventories.

The future challenges that must be addressed to improve AID-FOREST include (i) developing new algorithms to cope with estimation of the total stem volume for sympodial trees; (ii) defining additional processes for classifying stem wood in the possible merchantable wood products; and (iii), the most ambitious point, identifying different tree species, or at least groups within the genera, when using point clouds. Regarding the latter, Othmani et al. (2013) proposed a method for species detection based on a point cloud generated with TLS. They suggested using multiresolution analysis of the geometric texture of the bark together with software leveraging the Random Forest algorithm for classification. However, the results obtained by this group to date have been poor.

#### 5. Conclusions

Here we presented a new framework for forest inventorying based on point clouds processed with AID-FOREST software. In this work, point clouds were recorded using a hand-held terrestrial laser scanner (MTLS, ZEB-HORIZON, Geoslam Ltd.) and their processing was conducted with AID-FOREST. This software takes a hitherto unused approach to detect trees by leveraging an artificial intelligence algorithm. AID-FOREST

demonstrated a high level of tree detection (an average of 97 %), and only did not reach 100 % on some plots as a consequence of the high visual complexity of the ecosystem (EVCI). Detection did not depend on the tree species, stand density, or plot size, which makes the software widely applicable.

Moreover, AID-FOREST was statistically unbiased in terms of plot level accuracy at the mean DBH; in other words, the BIAS (0.6 cm, 1.8 %) was not statistically significantly different to 0. In addition, the DBH distribution function was not significantly different from the distribution function obtained by our field measurements. Indeed, estimations at the tree level showed that both the DBH and total tree volume (Vt) were unbiased compared to accurate field measurements. The relative BIAS was 0.16 % and – 1.37 %, respectively for DBH and Vt, and these values were not significantly different to 0. However, for total tree height, there was a BIAS of – 1.33 m (overestimation) because of the different concept of total height used in the field measurements and AID-FOREST estimations.

In conclusion, the main characteristics that differentiate this software from other solutions are that AID-FOREST (i) is totally automatic once launched; (ii) can process point cloud files of very large size; (iii) it processes \*.las files relatively quickly; and (iv) it outputs multiple useful and accurate dendrometric and forest stand parameters in different formats (as \*.shp and \*.csv files). Consequently, AID-FOREST is a robust, efficient and accurate software that extracts all the main forest stand parameters of a site, thereby helping to optimise sustainable forest stand management. Nevertheless, AID-FOREST still requires some additional improvements such as including species not mentioned in this paper and resolving the problem of calculating the total volume of the multiple stems of sympodial trees.

## Declaration of Competing Interest

The authors declare that they have no known competing financial interests or personal relationships that could have appeared to influence the work reported in this paper.

## Data availability

Data will be made available on request.

## Acknowledgments

This work was co-financed by the Spanish Ministry of Agriculture, Fisheries and Food and the European Agricultural Fund for Rural Development (FEADER) for the execution of innovation projects of general interest by operational groups (the Digital Forest Operational Group, ref. 2018 0020012125) of the European Association for Innovation in Agricultural Productivity and Sustainability (AEI-AGRI), and by the National Program for Fundamental Research Projects and National Program for Research, Development and Innovation Oriented to the Challenges of Society (CGL2017-83538-C3; PID2020-119861RB-I00; SBPLY/19/180501/000322). We also appreciate the accommodations granted to us by the Ministry of Agriculture, Rural Development, Climate Emergency and Ecological Transition of the Valencian Community, of the Autonomous Community of Castilla-La Mancha, as well as the Government of Navarra, the Forestry and Hunting Service, and Forest Guardianship Service to conduct this field work. We are grateful for the field work carried out by the BASARTEA S.L. as well as for their evaluation and application of AID-FOREST, to GRAFINTA S.L. for the technical support in managing the ZEB-HORIZON, Geoslam HUB and DRAW software, ENCE (National Company of Cellulose) for data collection in their own forests, and the students from the CIFP Aguas Nuevas (Albacete) for help with this field work. Finally, we would like to thank the University of Castilla-La Mancha, Spain, for the funds they granted us for this work.

## Appendix A. Supplementary material

Supplementary data to this article can be found online at <https://doi.org/10.1016/j.jag.2022.103014>.

## References

- Apostol, B., Chivulescu, S., Ciceu, A., Petriță, M., Pascu, I.-S., Apostol, E.N., Leca, S., Lorent, A., Tanase, M., Badea, O., 2018. Data collection methods for forest inventory: a comparison between an integrated conventional equipment and terrestrial laser scanning. *Ann. For. Res.* 61, 189–202.
- Barba, S., di Filippo, A., Limongiello, M., Messina, B., 2019. Integration of active sensors for geometric analysis of the chapel of the holy shroud. *Int. Arch. Photogramm. Remote Sens. Spatial Inf. Sci.* XLII-2/W15, 149–156.
- Bauwens, S., Bartholoméus, H., Calders, K., Lejeune, P., 2016. Forest inventory with terrestrial LiDAR: a comparison of static and hand-held mobile laser scanning. *Fores.* 7.
- Bienert, A., Scheller, S., Keane, E., Mohan, Nugent, C., 2007. Tree detection and diameter estimations by analysis of forest terrestrial laser scanner point clouds. In: ISPRS Workshop on Laser Scanning 2007 and SilviLaser.
- Bienert, A., Georgi, L., Kunz, M., Maas, H.-G., von Oheimb, G., 2018. Comparison and combination of mobile and terrestrial laser scanning for natural forest inventories. *Fores.* 9.
- Bogdanovich, E., Pérez-Priego, O., El-Madany, T.S., Guderle, M., Pacheco-Labrador, J., Levick, S.R., Moreno, G., Carrara, A., Pilar Martín, M., Migliavacca, M., 2021. Using terrestrial laser scanning for characterizing tree structural parameters and their changes under different management in a Mediterranean open woodland. *For. Ecol. Manage.* 486.
- Cabo, C., Ordoñez, C., García-Cortés, S., Martínez, J., 2014. An algorithm for automatic detection of pole-like street furniture objects from Mobile Laser Scanner point clouds. *ISPRS J. Photogramm. Remote Sens.* 87, 47–56.
- Cabo, C., Del Pozo, S., Rodríguez-Gonzálvez, P., Ordóñez, C., González-Aguilera, D., 2018b. Comparing terrestrial laser scanning (TLS) and wearable laser scanning (WLS) for individual tree modeling at plot level. *Remote Sens.* 10.
- Cabo, C., Ordóñez, C., López-Sánchez, C.A., Armesto, J., 2018b. Automatic dendrometry: Tree detection, tree height and diameter estimation using terrestrial laser scanning. *Int. J. Appl. Earth Obs. Geoinf.* 69, 164–174.
- Chen, D., Li, J., Di, S., Peethambaran, J., Xiang, G., Wan, L., Li, X., 2021. Critical points extraction from building façades by analyzing gradient structure tensor. *Remote Sens.* 13.
- Chen, S., Liu, H., Feng, Z., Shen, C., Chen, P., 2019. Applicability of personal laser scanning in forestry inventory. *PLoS ONE* 14, e0211392.
- Del Perugia, B., Giannetti, F., Chirici, G., Travaglini, D., 2019. Influence of scan density on the estimation of single-tree attributes by hand-held mobile laser scanning. *Fores.* 10.
- Dewez, T.J.B., Yart, S., Thuon, Y., Pannet, P., Plat, E., 2017. Towards cavity-collapse hazard maps with Zeb-Revo handheld laser scanner point clouds. *Photogram. Rec.* 32, 354–376.
- Donager, J.J., Sánchez Meador, A.J., Blackburn, R.C., 2021. Adjudicating perspectives on forest structure: how do airborne, terrestrial, and mobile lidar-derived estimates compare? *Remote Sens.* 13.
- Gollob, C., Ritter, T., Nothdurft, A., 2020. Forest inventory with long range and high-speed personal laser scanning (PLS) and simultaneous localization and mapping (SLAM) technology. *Remote Sens.* 12.
- Gorte, B., Pfeifer, N., 2004. Structuring laser-scanned trees using 3D mathematical morphology.
- Gorte, B.G.H., Winterhalder, D., 2004. Reconstruction of laser-scanned trees using filter operations in the 3D-raster domain. *Int. Arch. Photogramm. Remote Sens. Spatial Inf. Sci.* 36, 39–44.
- Heinzel, J., Huber, M.O., 2017. Detecting tree stems from volumetric TLS data in forest environments with rich understory. *Remote Sens.* 9, 9.
- Heo, H.K., Lee, D.K., Park, J.H., Thorne, J.H., 2019. Estimating the heights and diameters at breast height of trees in an urban park and along a street using mobile LiDAR. *Landscape Ecol. Eng.* 15, 253–263.
- Holopainen, M., Väistänta, M., Hyppä, J., 2014. Outlook for the next generation's precision forestry in Finland. *Fores.* 5, 1682–1694.
- Hosoi, F., Nakai, Y., Omasa, K., 2013. 3-D voxel-based solid modeling of a broad-leaved tree for accurate volume estimation using portable scanning lidar. *ISPRS J. Photogramm. Remote Sens.* 82, 41–48.
- Huang, J., Rathod, V., Sun, C., Zhu, M., Korattikara, A., Fathi, A., Fischer, I., Wojna, Z., Song, Y., Guadarrama, S., 2017. Speed/accuracy trade-offs for modern convolutional object detectors. In: Proceedings of the IEEE conference on computer vision and pattern recognition, pp. 7310–7311.
- Hyppä, E., Hyppä, J., Hakala, T., Kukko, A., Wulder, M.A., White, J.C., Pyörälä, J., Yu, X., Wang, Y., Virtanen, J.-P., Pohjavirta, O., Liang, X., Holopainen, M., Kaartinen, H., 2020a. Under-canopy UAV laser scanning for accurate forest field measurements. *ISPRS J. Photogramm. Remote Sens.* 164, 41–60.
- Hyppä, E., Kukko, A., Kaijaluoto, R., White, J.C., Wulder, M.A., Pyörälä, J., Liang, X., Yu, X., Wang, Y., Kaartinen, H., Virtanen, J.-P., Hyppä, J., 2020b. Accurate derivation of stem curve and volume using backpack mobile laser scanning. *ISPRS J. Photogramm. Remote Sens.* 161, 246–262.
- Liang, X., Kukko, A., Kaartinen, H., Hyppä, J., Yu, X., Jaakkola, A., Wang, Y., 2014. Possibilities of a personal laser scanning system for forest mapping and ecosystem services. *Sensors* 14, 1228–1248.

- Liang, X., Kankare, V., Hyypä, J., Wang, Y., Kukko, A., Haggrén, H., Yu, X., Kaartinen, H., Jaakkola, A., Guan, F., Holopainen, M., Vastaranta, M., 2016. Terrestrial laser scanning in forest inventories. *ISPRS J. Photogramm. Remote Sens.* 115, 63–77.
- Liang, X., Kukko, A., Hyypä, J., Lehtomäki, M., Pyörälä, J., Yu, X., Kaartinen, H., Jaakkola, A., Wang, Y., 2018. In-situ measurements from mobile platforms: an emerging approach to address the old challenges associated with forest inventories. *ISPRS J. Photogramm. Remote Sens.* 143, 97–107.
- Liang, H., Li, P., Cao, C., Yang, S., 2021. Analysis and monitoring technology of upper seam mining in multiunderlayer goaf. *Adv. Civil Eng.* 2021, 1–10.
- Liang, X., Wang, Y., Pyörälä, J., Lehtomäki, M., Yu, X., Kaartinen, H., Kukko, A., Honkavaara, E., Issaoui, A.E.I., Nevalainen, O., Vaaja, M., Virtanen, J.-P., Katoh, M., Deng, S., 2019. Forest in situ observations using unmanned aerial vehicle as an alternative of terrestrial measurements. *For. Ecosyst.* 6.
- Mengesha, T., Hawkins, M., Nieuwenhuis, M., 2015. Validation of terrestrial laser scanning data using conventional forest inventory methods. *Eur. J. Forest Res.* 134, 211–222.
- Mokroš, M., Mikita, T., Singh, A., Tomašík, J., Chudá, J., Węzyk, P., Kuželka, K., Šurový, P., Klímánek, M., Zięba-Kulawik, K., Bobrowski, R., Liang, X., 2021. Novel low-cost mobile mapping systems for forest inventories as terrestrial laser scanning alternatives. *Int. J. Appl. Earth Obs. Geoinf.* 104.
- Næsset, E., 2002. Predicting forest stand characteristics with airborne scanning laser using a practical two-stage procedure and field data. *Remote Sens. Environ.* 80, 88–99.
- Nelson, R., Parker, G., Hom, M., 2003. A portable airborne laser system for forest inventory. *Photogramm. Eng. Remote Sens.* 69, 267–273.
- Neter, J., Kutner, M.H., Nachtsheim, C.J., Wasserman, W., 1996. Applied Linear Statistical Models, fourth ed., Irwin, Chicago.
- Olofsson, K., Holmgren, J., Olsson, H., 2014. Tree stem and height measurements using terrestrial laser scanning and the RANSAC algorithm. *Remote Sens.* 6, 4323–4344.
- Othmani, A., Piboule, A., Krebs, M., Stolz, C., LewYan Voon, L.F.C., 2011. Towards automated and operational forest inventories with T-Lidar. In: 11th International Conference on LiDAR Applications for Assessing Forest Ecosystems (SilviLaser). HALL Hobart, Australia.
- Othmani, A., Lew Yan Voon, L.F.C., Stolz, C., Piboule, A., 2013. Single tree species classification from Terrestrial Laser Scanning data for forest inventory. *Pattern Recognition Lett.* 34, 2144–2150.
- Pardé, J., Bouchon, J., 1994. Dasometría. Versión española de Dendrométrie. École Nationale de Génie Rural des Eaux et Forêts (ENGREF), Madrid.
- Patrucco, G., Rinaudo, F., Spreafico, A., 2019. Multi-source approaches for complex architecture documentation: the “Palazzo Ducale” in Gubbio (Perugia, Italy). *Int. Arch. Photogramm. Remote Sens. Spatial Inf. Sci.* XLII-2/W11, 953–960.
- Pfeifer, N., Winterhalder, D., 2004. Modelling of tree cross sections from terrestrial laser-scanning data with free-form curves. *Int. Arch. Photogramm. Remote Sens. Spatial Inf. Sci.* 36, 76–81.
- Rastiveis, H., Shams, A., Sarasua, W.A., Li, J., 2020. Automated extraction of lane markings from mobile LiDAR point clouds based on fuzzy inference. *ISPRS J. Photogramm. Remote Sens.* 160, 149–166.
- Raumonen, P., Kaasalainen, M., Åkerblom, M., Kaasalainen, S., Kaartinen, H., Vastaranta, M., Holopainen, M., Disney, M., Lewis, P., 2013. Fast automatic precision tree models from terrestrial laser scanner data. *Remote Sens.* 5, 491–520.
- Raval, S., Banerjee, B.P., Singh, S.K., Canbulat, I., 2019. A preliminary investigation of mobile mapping technology for underground mining. In: IGARSS 2019–2019 IEEE International Geoscience and Remote Sensing Symposium. IEEE, pp. 6071–6074.
- Ren, S., He, K., Girshick, R., Sun, J., 2015. Faster r-cnn: towards real-time object detection with region proposal networks. *Adv. Neural Inf. Process. Syst.* 28.
- Rodriguez-Martin, M., Rodriguez-Gonzalvez, P., Gonzalez-Aguilera, D., Nocerino, E., 2018. Novel approach for three-dimensional integral documentation of machine rooms in hospitals using portable mobile mapping system. *IEEE Access* 6, 79200–79210.
- Russakim, N.A.S., Ariff, M.F.M., Darwin, N., Majid, Z., Idris, K.M., Abbas, M.A., Zainuddin, N.K., Yusoff, A.R., 2018. The suitability of terrestrial laser scanning for strata building, the international archives of the photogrammetry, Remote Sens. Spatial Inf. Sci. XLII-4/W9, 67–76.
- Ryding, J., Williams, E., Smith, M., Eichhorn, M., 2015. Assessing handheld mobile laser scanners for forest surveys. *Remote Sens.* 7, 1095–1111.
- Safaie, A.H., Rastiveis, H., Shams, A., Sarasua, W.A., Li, J., 2021. Automated street tree inventory using mobile LiDAR point clouds based on Hough transform and active contours. *ISPRS J. Photogramm. Remote Sens.* 174, 19–34.
- Serra, J., 1982. Image Analysis and Mathematical Morphology. Academic Press, London.
- Shams, A., Sarasua, W.A., Famili, A., Davis, W.J., Ogle, J.H., Cassule, L., Mammadrahimli, A., 2018. Highway Cross-Slope Measurement using Mobile LiDAR. *Transp. Res. Record: J. Transp. Res. Board* 2672, 88–97.
- Shinozaki, K., Yoda, K., Hozumi, K., Kira, T., 1964a. A quantitative analysis of plant form-the pipe model theory: I. Basic analyses. *Jpn. J. Ecol.* 14, 97–105.
- Shinozaki, K., Yoda, K., Hozumi, K., Kira, T., 1964b. A quantitative analysis of plant form-the pipe model theory: II. Further evidence of the theory and its application in forest ecology. *Jpn. J. Ecol.* 14, 133–139.
- Shokri, D., Rastiveis, H., Shams, A., Sarasua, W.A., 2019. Utility poles extraction from mobile lidar data in urban area based on density information. *Int. Arch. Photogramm. Remote Sens. Spatial Inf. Sci.* XLII-4/W18, 1001–1007.
- Simonse, M., Aschoff, T., Spiecker, H., Thies, M., 2003. Automatic determination of forest inventory parameters using terrestrial lasercanning. In: Proceedings of the ScandLaser Scientific Workshop on Airborne Laser Scanning of Forests, Umeå, Sweden, pp. 251–257.
- Topolsek, D., Herbaj, E.A., Kamnik, R., 2019. 3D laser scanners and point clouds for obtaining car accident sketches. *Revija za kriminalistiko in kriminologijo/Ljubljana* 70, 335–351.
- Van Leeuwen, M., Nieuwenhuis, M., 2010. Retrieval of forest structural parameters using LiDAR remote sensing. *Eur. J. Forest Res.* 129, 749–770.
- Vatandaşlar, C., Zeybek, M., 2020. Application of handheld laser scanning technology for forest inventory purposes in the NE Turkey. *Turk. J. Agric. For.* 44, 229–242.
- Vatandaşlar, C., Zeybek, M., 2021. Extraction of forest inventory parameters using handheld mobile laser scanning: a case study from Trabzon, Turkey. *Measurement* 177.
- Yang, B., Fang, L., Li, J., 2013. Semi-automated extraction and delineation of 3D roads of street scene from mobile laser scanning point clouds. *ISPRS J. Photogramm. Remote Sens.* 79, 80–93.
- Zheng, Y., Peter, M., Zhong, R., Oude Elberink, S., Zhou, Q., 2018. Space subdivision in indoor mobile laser scanning point clouds based on scanline analysis. *Sensors (Basel)* 18.